A temporal analysis of East Pacific and East Atlantic ship-tracks

Millman, Thomas M.

Monterey, California. Naval Postgraduate School

Approved for public release; distribution is unlimited.

A Temporal Analysis of East Pacific and East Atlantic Ship-Tracks

by

Thomas M. Millman
Lieutenant, United States Navy
B.S., U.S. Naval Academy, 1986

Submitted in partial fulfillment
of the requirements for the degree of

MASTER OF SCIENCE IN METEOROLOGY AND PHYSICAL OCEANOGRAPHY

from the

NAVAL POSTGRADUATE SCHOOL
December 1992

ECURITY CLASSIFICATION OF THIS PAGE

REPORT DOCUMENTATION PAGE

a. REPORT SECURITY CLASSIFICATION INCLASSIFIED	1b. RESTRICTIVE MARKINGS
a. SECURITY CLASSIFICATION AUTHORITY	3. DISTRIBUTION/AVAILABILITY OF REPORT Approved for public release; distribution is unlimited.
b. DECLASSIFICATION/DOWNGRADING SCHEDULE	
. PERFORMING ORGANIZATION REPORT NUMBER(S)	5. MONITORING ORGANIZATION REPORT NUMBER(S)
a. NAME OF PERFORMING ORGANIZATION Naval Postgraduate School 6b. OFFICE SYMBOL (*If applicable*) 35	7a. NAME OF MONITORING ORGANIZATION Naval Postgraduate School
c. ADDRESS (*City, State, and ZIP Code*) Monterey, CA 93943-5000	7b. ADDRESS (*City, State, and ZIP Code*) Monterey, CA 93943-5000
a. NAME OF FUNDING/SPONSORING ORGANIZATION 8b. OFFICE SYMBOL (*If applicable*)	9. PROCUREMENT INSTRUMENT IDENTIFICATION NUMBER
c. ADDRESS (*City, State, and ZIP Code*)	10. SOURCE OF FUNDING NUMBERS Program Element No / Project No. / Task No. / Work Unit Accession Number

11. TITLE (*Include Security Classification*)

A TEMPORAL ANALYSIS OF EAST PACIFIC AND EAST ATLANTIC SHIP TRACKS (UNCLAS)

12. PERSONAL AUTHOR(S) THOMAS M. MILLMAN

13a. TYPE OF REPORT	13b. TIME COVERED	14. DATE OF REPORT (*year, month, day*)	15. PAGE COUNT
Master's Thesis	From To	DECEMBER 1992	76

16. SUPPLEMENTARY NOTATION

The views expressed in this thesis are those of the author and do not reflect the official policy or position of the Department of Defense or the U.S. Government.

17. COSATI CODES			18. SUBJECT TERMS (*continue on reverse if necessary and identify by block number*)
FIELD	GROUP	SUBGROUP	METEOROLOGY. SPATIAL, TEMPORAL AND RADIATIVE PROPERTIES OF SHIP TRACKS

19. ABSTRACT (*continue on reverse if necessary and identify by block number*)

The spatial, temporal and radiative properties of ship tracks are described with an analysis of AVHRR (Advanced Very High Resolution Radiometer) imagery. 15 cases are analyzed including 6 from the Atlantic Stratocumulus Transition Experiment (ASTEX) in the Azores islands, from ship tracks observed off the coast of Oregon and 3 from the 1987 First ISCCP (International Satellite Cloud Climatology Project) Regional Experiment (FIRE) (Starr, 1987). The reflectance in channel 3 (3.7 microns) of each ship track and associated background are analyzed as a function of time. The width of each ship track is also plotted as a function of time to determine their spatial and dispersive qualities. The eastern Pacific Ocean ship tracks are generally less dispersive, but two ASTEX ship tracks were more dispersive than what would be consistent over land. In individual cases, higher ambient reflectances are associated with environments that are less sensitive to ship effluent resulting in lower ship track reflectances. But in the composite of all ship track cases, higher ambient reflectances are associated with environments that are more sensitive to ship effluent resulting in higher ship track reflectances. Though the number of cases was limited due to weather and other phenomena, the reflectance, width and dispersion analysis highlight the commonalities and differences between the ship tracks from the two areas. This indicates that the state of the atmosphere has a substantial effect on ship track formation.

20. DISTRIBUTION/AVAILABILITY OF ABSTRACT	21. ABSTRACT SECURITY CLASSIFICATION	
☒ UNCLASSIFIED/UNLIMITED ☐ SAME AS REPORT ☐ DTIC USERS	UNCLASSIFIED	
22a. NAME OF RESPONSIBLE INDIVIDUAL PHILIP A. DURKEE	22b. TELEPHONE (*Include Area code*) (408)646-3465	22c. OFFICE SYMBOL 64/De

DD FORM 1473, 84 MAR 83 APR edition may be used until exhausted
All other editions are obsolete

SECURITY CLASSIFICATION OF THIS PAGE
UNCLASSIFIED

ABSTRACT

The spatial, temporal and radiative properties of ship tracks are described with an analysis of AVHRR (Advanced Very High Resolution Radiometer) imagery. 15 cases are analyzed including 6 from the Atlantic Stratocumulus Transition Experiment (ASTEX) in the Azores islands, 6 from ship tracks observed off the coast of Oregon and 3 from the 1987 First ISCCP (International Satellite Cloud Climatology Project) Regional Experiment (FIRE) (Starr, 1987). The reflectance in channel 3 (3.7 microns) of each ship track and associated background are analyzed as a function of time. The width of each ship track is also plotted as a function of time to determine their spatial and dispersive qualities. The east Pacific Ocean ship tracks are generally less dispersive, but two ASTEX ship tracks were more dispersive than what would be consistent over land. In individual cases, higher ambient reflectances are associated with environments that are less sensitive to ship effluent resulting in lower ship track reflectances. But in the composite of all ship track cases, higher ambient reflectances are associated with environments that are more sensitive to ship effluent resulting in higher ship track reflectances. Though the number of cases was limited due to weather and other phenomena, the reflectance, length and dispersion analysis highlight the commonalities and differences between the ship tracks from the two areas. This indicates that the state of the atmosphere has a substantial effect on ship track formation.

TABLE OF CONTENTS

ACKNOWLEDGEMENTS

Though neither time nor space permits me to truly thank all the people who have assisted me in this undertaking, however I would like to express my gratitude to a few of them.

First, I would like to thank Mr. Craig Motell for his assistance in processing images in the Azores. I hope he's enjoying life in Hawaii.

Secondly, to Mr. Kurt Nielsen whose acumen for programming and ready smile not only eased my work load significantly, but also energized my spirits when the road ahead looked tough.

I would also like to thank Mr. Chuck Skupniewicz for his assistance in understanding the dispersion properties of "puffs" of clouds and ship tracks.

Mr. Jim Cowie provided me with the nuances of plotting and graphing in the IDEA lab that probably only he knows.

A note of appreciation to my fellow students whom I enjoyed both professionally and personally. I look forward to seeing them again soon in the "real world."

Finally, I am grateful to Dr. Carlyle H. Wash and especially to Dr. Philip A. Durkee. Dr. Durkee's friendly "pushes" and guidance were invaluable. Despite his very hectic schedule, Dr. Durkee still made himself available for consultation whenever the situation arose and provided me with the confidence to finally tie it all together at the end. Thanks Phil!

1. INTRODUCTION

Ship tracks are regarded with considerable interest and at times bewilderment. We know that they occur and understand relatively well their structure, but cannot yet completely solve their dynamics. Initially observed by Conover (1966), they have since piqued the curiousity of scientists.

Ship tracks have been analyzed by various approaches in the hopes of identifying their formation mechanisms. These cloud anomalies are characterized by an increase in droplet concentration and a corresponding decrease in droplet size (Twomey and Cocks, 1982). The smaller droplets result in higher reflectance in the channel 3 NOAA AVHRR imagery. However, the spatial and radiative properties of ship tracks are not well understood.

There are several motivations for ship track analysis. Military applications demand an understanding of their mechanisms, and how to deter their formation. Commercial fisheries have a vested interest in ship track analysis to protect fisheries. Meteorologically, ship tracks will also help us to further understand turbulence and boundary layer phenomena.

The most concentrated ship track research has been off the coast of California. Here the ship track signature is relatively frequent due to the predominance of stratiform clouds. Yet these cloud types are present in other parts of the world as well and ship tracks can be expected to produce different signatures. Salvato (1992) noted that Arctic ship tracks have a relatively stronger signature than ship tracks observed in the eastern Pacific Ocean. It has been speculated that differences in the boundary layer contribute to the differences seen in the strength of ship tracks.

This thesis will focus on a comparison of ship tracks from the eastern Pacific and eastern Atlantic Oceans. Recently, the ASTEX (Atlantic Stratocumulus Transition Experiment) was performed in the Azores islands. These islands are located approximately 1000 miles west of Portugal. The period of study for this experiment was 24 days-from 4 June to 28 June 1992. Another exercise was recently conducted off the coast of Oregon in August 1992 and again studied ship tracks. Finally, ship tracks will be analyzed from the 1987 FIRE experiment conducted off the coast of southern California. This thesis will compare and contrast the ship tracks from these two regions of the world. By utilizing the Nielsen and Durkee algorithm (1992), information on ship track length, width, persistence and spatial and radiative characteristics will be extracted and compared for the two areas.

II. THEORY

A. CLOUD MICROPHYSICS

Morehead (1988) describes scattering and absorption as two interactions that electromagnetic energy can undergo when transiting the atmosphere. Three processes that occur with these two interactions are emission, reflectance and transmittance. They are governed by the conservation equation:

$$\varepsilon + \rho + \tau = 1$$

where ε is emission, ρ is reflectance by scattering and τ is transmittance. Since reflectance by scattering is the domintant interaction of solar energy by clouds. transmittance and emission will not be discussed further.

1. Scattering

As described by Morehead (1988), scattering by clouds is dependent upon several factors but the ones relevant to this discussion are particle size distribution and particle composition. At the visible and IR wavelengths considered in this analysis, Mie scattering will be the primary scattering mechanism.

2. Aerosol distribution

There are a variety of types of aerosols. They can range in size from cloud condensation nuclei or CCN which are on the order of .1μm radius to large cloud droplets that may have radius up to 100μm. The degree of scattering and consequently reflectance will be a function of the size and concentration of the scatters. There are also differences in the wavelengths measured. Channel 1 (.63 microns) and channel 3 (3.7 microns) are depicted in Figures 1 and 2 respectively. Channel 1 reflectance is a function of both liquid water path and particle size while channel 3 reflectance is a function of particle size only. Therefore, since ship track reflectance is dependent primarily upon particle size, channel 3 will provide the most accurate representation of the track reflectance.

Though there are many souces of aerosols, the focus here will be on those from ships' exhausts. Ships inject aerosols into the atmosphere increasing the number that are available as CCN, and since the CCN distribution determines the cloud droplet distribution, this will subsequently lead to higher values in droplet concentration. These changes were examined by Twomey and Cocks (1982). The jump in droplet concentration is coupled with a decrease in droplet size. A key point here is that the ship's exhaust does not substantially alter the cloud's liquid water content in a given volume of atmosphere. The increase in droplet concentration and decrease in droplet size equates to an increase in reflectence due to scattering as demonstrated by Twomey (1977).

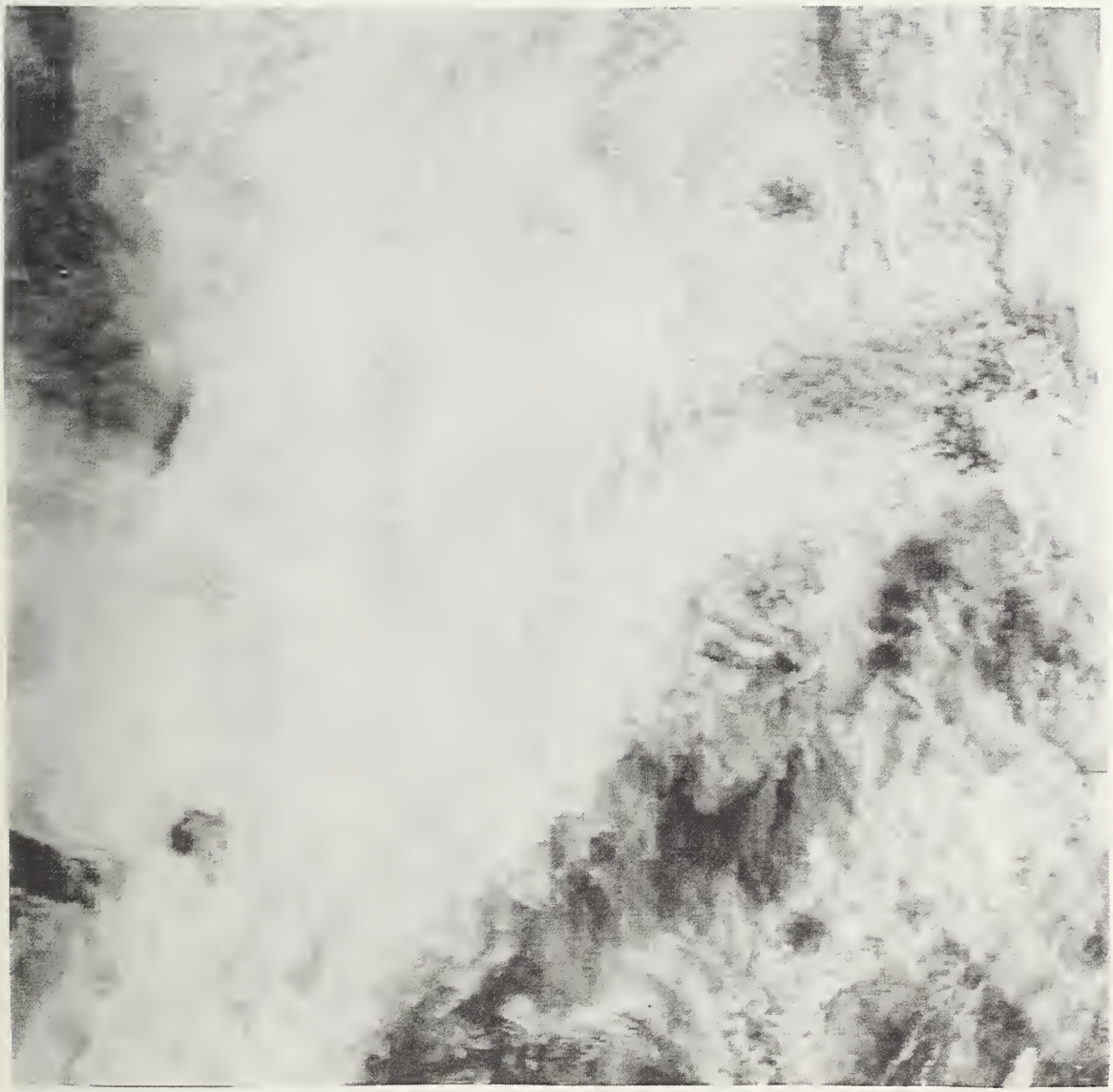

Figure 1. Channel 1(Visible) satellite imagery showing ship-tracks at 0903Z on 14 June 1992

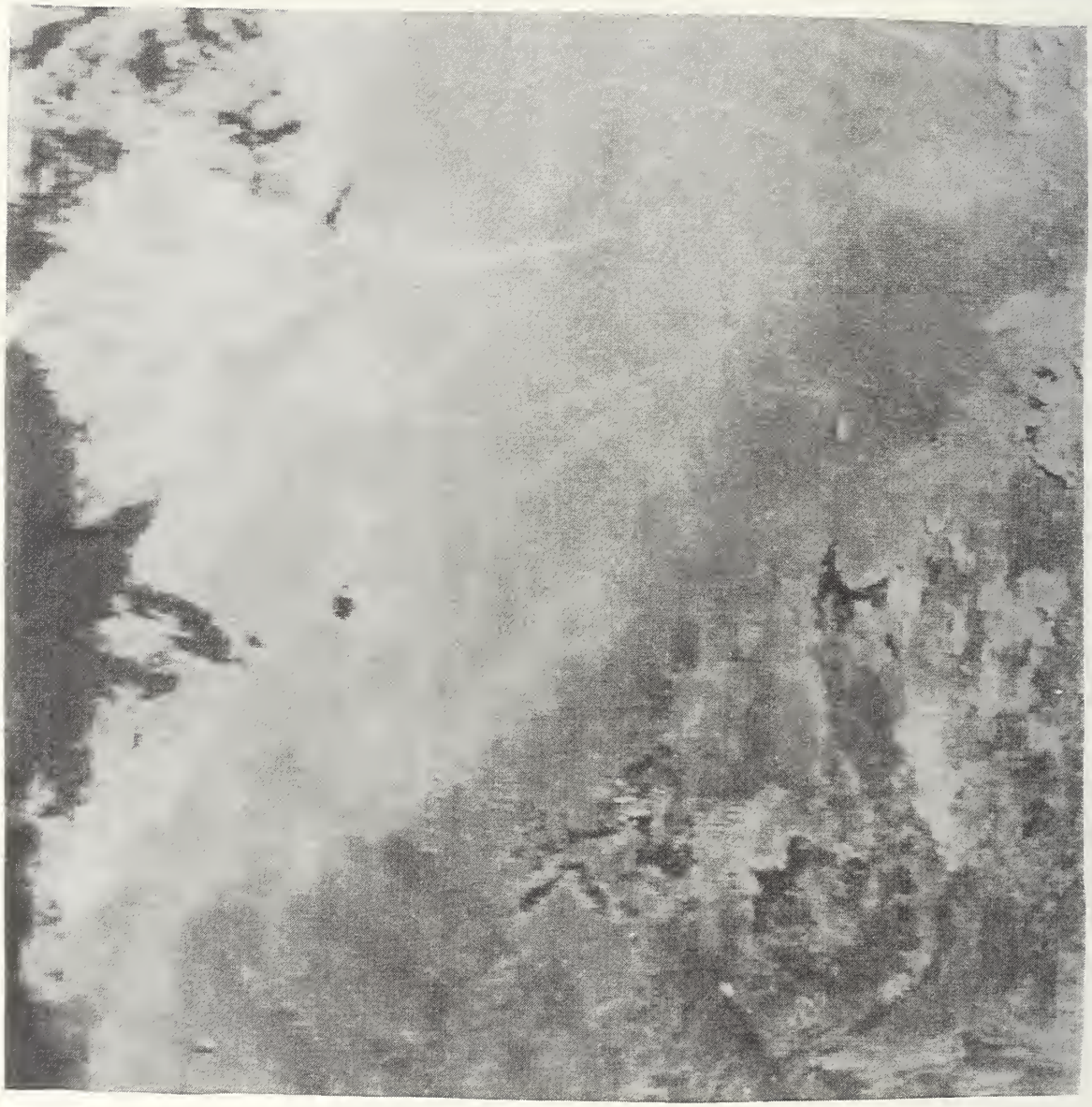

Figure 2. Channel 3(Infrared) satellite imagery showing ship-track at 0903Z on 14 June 1992

III. PROCEDURE AND PROCESSING

Chapter III describes the NOAA satellites and sensor that was used to collect data. This section will also detail data processing including the procedures and criteria for analyzing the ship tracks.

A. THE SATELLITE AND SENSOR

The NOAA 10, 11 and 12 polar orbiting satellites were the platforms utilized to gather the imagery for this thesis.. These satellites operate in a sun-synchronous orbit at an altitude of 525 miles. They provided coverage of the Azores region eight times daily.

The image sensor aboard the satellite was the Advanced Very High Resolution Radiometer (AVHRR) instrument. It can collect radiance in 5 channels although only channel 3 (3.7 microns) was used. The resolution of this sensor is 1km by 1km at nadir.

B. PROCESSING

The data from ASTEX and off the coast of Oregon were received and processed by a High Resolution Picture Transmission (HRPT) ground station developed by Global Imaging. The channels 1-5 images could be displayed directly. But but primarily channels 1 and 3 were analyzed using the Nielsen and Durkee algorithm (1992) on the Interactive Digital Environmental Analysis (IDEA) laboratory at the Naval Postgraduate School . The algorithm products

for this thesis include the channel 3 reflectance scaled by the zenith angle (called LOW3). In the analysis ambient reflectance is labeled LOW3A and ship track reflectance is called LOW3B. Also produced is the difference in reflectance ($\Delta\rho$) between the ship track and the background, i.e.ship track minus background reflectance. For the most part, ship track reflectance should exceed background reflectance so the $\Delta\rho$ values will be positive. This may not be true on the very edge of the track where the background could potentially exceed the track reflectance.

Fifty images were studied for potential ship track candidates. A lack of ship correlation to ship tracks and unfavorable weather conditions limited the number of cases to 15.

There were two crucial processing steps to this discussion. The first was the ability to convert the length of the ship track to a function of time. To determine this quantity a vector relationship for the relative wind was utilized similar to Pettigrew (1992). Specifically, the ship's course and speed and the true wind were needed. The course and speed of the ship were calculated using two successive images. The course is simply taken as the bearing between ship track heads on successive satellite overpasses. The speed is the distance between ship track heads divided by the difference in time between satellite overpasses. An estimate of the true wind was obtained from the National Meteorological Center (NMC) Spectral Gridded Model (SGM) wind analysis as a function of height and at various locations. This true wind was then compared with surface wind in the Azores for the ASTEX cases and observations made off the coast of Oregon for those cases. The estimated true wind and observed true wind from observations often differed. Therefore, the final criteria for selecting the true

wind was that the bearing of the calculated relative wind would have to match or closely approximate the direction of the ship track. To complete the problem, a time was derived by measuring the length of the track and dividing by the relative wind speed. For cases from Pettigrew (1992), a relative wind was already available.

The second step was determining the width of the tracks at various points along the length. To accomplish this the ship track image was loaded in the IDEA lab and the specific function, pixel value (pixval) was employed. Pixval provides x and y image location and a digital value of any pixel in the image. By visually identifying the edges of the track and then using the change in gray values between the backgound and ship track as a verification, the width could be determined. Since this is a manual technique there are fewer width points than other parameters along the track.

Three properties of ship tracks will be studied. First, the difference in reflectance between the ship track and ambient clouds, hereafter referred to as $\Delta \rho$, are plotted versus time. The $\Delta\rho$ should approach zero as the track reflectance converges to the background reflectance. The width as a function of time is also analyzed and it is expected that the width will increase in time due to dispersion. Since the resolution of the satellite imagery is at best 1 km, a 2 km width is necessary for identification of the track. Finally, the reflectance of both the ship track and background are plotted versus time. Normally, the track reflectance is somewhat higher than the background reflectance. But some cases will show significantly higher track reflectance where the environment is extremely sensitive to ship effluent resulting in an increasing $\Delta\rho$ with time.

IV. CASE STUDIES

Fifteen cases will be analyzed including 6 from off the Oregon coast, 6 from ASTEX and 3 from the FIRE experiment. Incorporated into each case will be a brief description of pertinent meteorological factors for that day.Each track is labeled by the call sign of the ship (if available) or the Julian day of the image. In the captions of the delta versus time diagrams, Delta refers to ship track minus ambient reflectance.

A. 3EJI5

The ship track associated with callsign 3EJI5 was observed at 1639Z on 7 July 1987 by a NOAA-10 satellite (Pettigrew, 1992). The channel 3 imagery for this ship track is shown in Figure 3. Figure 4 presents the $\Delta\rho$ and width of the ship track with respect to time. The reflectance difference decreases with time approaching zero at 250 minutes. However, there is a distinct spike at about 100 minutes. In Figure 5 both the ambient reflectance (top), and the ship track reflectance (bottom), show a similar spike at approximately 100 minutes. Figure 3 illustrates that the ship track passes through an area of higher reflectance that reaches its peak at 34.0N 136.3W. This area is particularly sensitive to ship exhaust so a distinct maximum occurs. The width (Figure 4) generally increases thoughout the track life.

B. ELBH9

The ship track associated with callsign ELBH9 was observed at 2303Z on 14 July 1987 by a NOAA-9 satellite. This ship is the Merchant Vessel Neptune

Agate, a container ship (Pettigrew, 1992).The channel 3 imagery for this ship track is shown in Figure 6. The $\Delta\rho$ (Figure 7, top) exhibits an isolated maximum at about 18 minutes and then is generally constant with frequent and large fluctuations. Both the ambient and ship track reflectance shown at the top and bottom of Figure 8 respectively, show an overall decline in reflectance with time. It can be seen from the channel 3 imagery (Figure 6) that the ship track enters an area of lower ambient reflectance at about 38.8N 136.2W shortly after the track begins. This would account for the increase in $\Delta\rho$ at approximately 18 minutes shown by Figure 7 (top). The width (Figure 7, bottom) is variable, but generally increases. This is probably due to local environmental changes in cloud structure.

C. 3ERV

The ship track with callsign 3ERV produced a track observed at 1604Z on 4 July 1987 by a NOAA-10 satellite. This ship is the Merchant Vessel Antonio, a general cargo ship (Pettigrew, 1992). The channel 3 imagery for this ship track is shown in Figure 9. The significant feature in $\Delta\rho$, Figure 10 (top), is the sharp drop and then upward spike at about 130 minutes. The drop is due to the less reflective areas observed in the vicinity of the track intersection at 25.9N 120.1W (Figure 9). Figure 11 (bottom) shows the spike in the ship track reflectance at 130 minutes. This spike is associated with the track intersection shown at 25.9N 120.1W in Figure 9. The width (Figure 10, bottom) indicates a large variability. There is a substantial width increase starting at about 70 minutes and ending at about 150 minutes. The varying nature would seem to be indicative of local environmental changes in the cloud structure.

D. 166AB

Ship track 166AB was observed on two successive satellite overpasses. The first was 0903Z on 14 June 1992 by a NOAA-12 satellite. The channel 3 view of this track is shown in Figure 12. Although no ship was identified with the ship track, the ship originating track AB was on a course of 063°T at 11.09 knots. On 14 June 1992 the true wind was estimated to be 344°T at 12.4 knots in the region of the Azores. Thus the relative wind was about 040°T at 14.6 knots. The head of this track is at point A. The significant feature of note in the $\Delta\rho$, shown at the Figure 13 (top), is the the jump in reflectance at about 180 minutes. The same spike is present in ship track reflectance at about 180 minutes (Figure 14, bottom). Figure 12 shows that the spike in ship track reflectance is correlated to the intersection with an unidentified track at 40N 26.2W. The ambient and ship track reflectances, Figure 14, indicate an increase in reflectance from about 270 minutes to 430 minutes. This corresponds well with the general increase in reflectance seen in the lower portion of the track as shown in Figure 12. The track width (Figure 13) shows two maxima at about 70 and 220 minutes respectively with a relative minima occurring at the 140 minute mark.

Ship track AB was again observed 7 hours on 14 June at 1625Z by a NOAA-11 satellite. Figure 15 shows the channel 3 imagery of the ship track with the head of the track at point A. The $\Delta\rho$ (Figure 16) shows an overall increase with time with large fluctuations. There are three possible explanations for the $\Delta\rho$ increase with time. The first is that the ship changes its speed, thus changing the amount of effluent it exhausts to the environment and ultimately affecting the reflectance. This is not likely since ships on long distance transits do not

normally change speeds. The second is that there is a gas-to-particle conversion that produces more aerosols with time acting to increase the ship track reflectance. However, there is not enough information here to substantiate this possibility. The third and most likely choice is that there is a change in environment. If the changing environment were more sensitive to ship effluent, then an increasing $\Delta\rho$ with time could result. The $\Delta\rho$ also exhibits a spike at about 100 minutes as does (Figure 17) the ship track reflectance. Figure 15 shows that track AB intersects track EF at about 100 minutes. This would account for the jump in ship track reflectance. The width of the track (Figure 16, bottom)does increase with time although there is an initial decrease from about 10 to 15 minutes.

E. 166 CD

The ship track called 166CD was observed also on two successive overpasses. The first was at 0903Z on 14 June 1992 by a NOAA-12 satellite. Figure 12 shows the channel 3 imagery for ship track 166CD. Although no ship was identified with track CD the course and speed for the ship originating track CD was about 221°T at 7.9 knots and the relative wind was about 304°T at 9.6 knots. The head of this ship track is at point C. The $\Delta\rho$ (Figure, top) exhibits an overall decrease over the life of the track. However, there is a substantial increase from 170 to 230 minutes. This corresponds very well with the increase in ship track reflectance at 200 minutes shown Figure 19 (bottom). The channel 3 imagery in Figure 12 explains this increase by indicating that track CD has a slight overlap with track AB at 40.5N 25.5W.

The reflectances exhibit unusual behavior in this case. The ambient and ship track reflectances (Figure 19) indicate a sharp boundary at 240 minutes with a sharp increase in reflectance. This boundary is indicative of a changing environment.

This track is a good example of the variable nature of Azores ship track widths (Figure 18, bottom). The explanation for this comes from the Azores having a relatively deeper boundary layer compared to the eastern Pacific Ocean. This higher thickness results in larger scale circlations where we have puffy cumulus clouds below a more uniform stratiform deck. These cumulus clouds induce the width variations. There is a narrowing of the track from 70 to 240 minutes. Normally this would be indicative of more smaller droplets and higher reflectances. However, because there is a track intersection in this case, the track narrowing is at best only a partial substantiation for the increase in track reflectance.

The second view of ship track CD is at 1625Z on 14 June 1992 by a NOAA-11 satellite. Figure 15 depicts the channel 3 imagery for this track. The head of the track is at point C. The top of Figure 20 shows the $\Delta\rho$. The $\Delta\rho$ has an overall increase with time indicating a changing environment that is more susceptible to ship effluent. There is one exception though and that is the strong dip at 120 minutes. This dip corresponds very well with the dip at 120 minutes in the ship track reflectance shown at the bottom of Figure 21. To tie this idea together, the channel imagery in figure 14 indicates a discontinuity in the ship track at 40N and 26.25W. There is a small spike at 135 minutes in both the ship track reflectance and the $\Delta\rho$. This is probably due to the intersection with track AB seen in the channel 3 imagery (Figure 15). The width shown at the bottom of

Figure 20 is constant through the middle of the formation period. The two increases at the beginning and end of the period indicate that there are large scale circulations inducing these frequent variations.

F. 166EF

Ship track 166EF was observed on two successive satellite overpasses. The first observation occurred at 0903Z on 14 June 1992 by a NOAA-12 satellite. The ship track is depicted in the channel 3 imagery (Figure 12) with its head at point E. Although no ship name was actually found with this track, the course and speed of the ship making the track was determined to be 241°T at 6.75 knots. The true wind was estimated to be 344°T at 12.4 knots while the relative wind was about 311°T at 12 knots. The $\Delta\rho$ (Figure 22, top) shows an overall decline with time although it is highly variable. There is a increase in brightness at 90 minutes that precedes a second upward spike at 110 minutes. The ship track reflectance (Figure 23, bottom) also shows these same features. The boundary and subsequent spike are possibly indicative of a changing environment that is more sensitive to ship effluent. The ambient reflectance (Figure 23, top) shows a similar boundary and spike, however they occur later and are not directly linked to to the boundary and spike in the $\Delta\rho$. The decline in ambient reflectance after 110 minutes undoubtedly contributes to the increase in the $\Delta\rho$. The track width (Figure 22, bottom) indicates two peaks to 7 kilometers with a dip to 3 kilometers in-between at 150 minutes. Although there is no evidence in the reflectance to account for this change, the fact that there are larger scale circulations in the Azores would provide an explanation for this variability.

The second observation of track EF occurred on 14 June 1992 at 1625Z by a NOAA-11 satellite. The channel 3 imagery for this ship track is presented in Figure 15 with the head of the track at point E. The $\Delta\rho$ (Figure 24, top) is highly variable with two important features. The first is the spike at 12 minutes. The ship track reflectance (Figure 25, bottom) indicates a similar jump at about 12 minutes. The ambient reflectance (Figure 25, top) indicates only small increases at 12 minutes. The channel 3 imagery (Figure 15) shows that track EF intersects track AB near its conception at the 12 minute mark. The second important feature in the $\Delta\rho$ (Figure 24, top) is the spike at 104 minutes to a peak of 7. Since the ambient reflectance is decreasing while the ship track reflectance is increasing in this area (Figure 25), this suggests that the ship entered an environment of high sensitivity to its effluent. The track width (Figure 24, bottom) is indicative of variable mixing. The width decline to 1 km at 80 minutes is consistent with the increase in the $\Delta\rho$ at the same time.

G. 239CD

Ship track CD was observed on three successive satellite overpasses. The first occurred at 1510Z on 26 August 1992 by a NOAA-10 satellite. Figure 26 depicts the ship track with the head of the ship track at point C. The ship originating track CD was the Forest Wave, a wood-chip carrier vessel with a oil-driven propulsion type (Freeberg, 1992). The ship was on a course of 292°T at a speed of 10.2 knots. The true wind on 26 August 1992 was estimated to be 012°T at 10.4 knots giving a relative wind of 331°T at 16.4 knots. The $\Delta\rho$ (Figure 27, top) starts at slightly negative values and then indicates an overall increase until the 84 minute mark. The negative $\Delta\rho$ values could be a result of

the noise in the NOAA-10 channel 3 data. The increase in $\Delta\rho$ indicates a changing environment that is more favorable to ship effluent. The ambient reflectance (Figure 28, top) exhibits an increase after 84 minutes. The cause for the increase in ambient reflectance and decrease in ship track reflectance at the end of the formation period is unknown. The width was unavailable because of noise in the NOAA-10 channel 3 data.

The second observation of track CD occurred at 1635Z by a NOAA-12 satellite. Figure 29 shows the ship track with the head of the track at point C. The $\Delta\rho$ (Figure 30, top) starts off at a value of 2.8 and after an initial decline to 5, reaches its maximum of 3.9 at 160 minutes. The same peak at 3.9 is present in the ship track reflectance at 160 minutes (Figure 31, bottom). Figure 29 shows that the reason for these peaks is the intersection between tracks CD and EF. The width (Figure 30, bottom) increases in a step-wise manner. The width increase is consistent with dispersion in that the track width shoud increase with time.

The final observation of track CD occurs at 2204Z by a NOAA-11 satellite. Figure 32 depicts the ship track with the head of the track at point C. The $\Delta\rho$ (Figure 33, top), indicates an overall increase from a value of .3 to a maximum value of 2.6. This implies that the changing environment is more sensitive to ship effluent. This is also consistent with the ambient and ship track reflectances depicted in Figure 34. The ambient reflectance (Figure 34, top) exhibits an overall decrease with time while the ship track reflectance (Figure 34, bottom) exhibits an overall increase with time, although the increase is variable. The width (Figure 33, bottom) exhibits an overall increase to 5 km after an initial decline from 4 to 3 km. The varying nature of the width is probably due to local environmental changes in the cloud structure.

H. 239EF

Ship track EF was observed on the same three successive satellite overpasses. The first occurred at 1510Z on 26 August 1992 by a NOAA-10 satellite. Figure 26 depicts the track with the head of track EF at point E. The ship originating track EF was the Al Alamira, a bulk cargo carrier with a oil-driven propulsion type (Freeberg, 1992). It was on a course of 292°T at a speed of 14.72 knots. The relative wind across its deck was 331°T at a speed of 15.8 knots. Figure 35 indicates that the $\Delta\rho$ is variable and increasing with time. The ambient and ship track reflectance (Figure 36) exhibit the same type of variability. This variability is probably due to local environmental changes. The width was unavailable because the track was on the pass edge.

The second observation of track EF occurred at 1635Z on 26 August 1992 by a NOAA-12 satellite with the head of the track at point E (Figure 29). The $\Delta\rho$ (Figure 37, top) exhibits an overall decrease with time after an initial increase to 3.2 at 35 minutes. The initial increase in the $\Delta\rho$ to a peak at 3.2 is probably due to an overlap with track CD. Figure 36 indicates this overlap at 46.4N 125.4W. The ship track reflectance (Figure 38, bottom) exhibits a peak value of 7.2 at 35 minutes. The decrease in the $\Delta\rho$ starting at 175 minutes indicates an increasing ambient reflectance. The ambient reflectance (Figure 38, top) does indeed increase at 175 minutes. Also, the channel 3 imagery (Figure 29), indicates an area of generally higher ambient reflectance towards the lower portion of track EF. The width (Figure 37, bottom)is varying with time. Although the width is variable, it exhibits an overall increase with time that is consistent with the decreasing $\Delta\rho$.

The final observation of track EF is at 2204Z by a NOAA-11 satellite (Figure 32). Although the $\Delta\rho$ (Figure 39, top) is variable, it does exhibit an overall increase with time. This is highlighted at 290 minutes where the ship track assumes greater influence in the reflectance. The ship track reflectance is relatively stronger than the ambient reflectance at 290 minutes (Figure 40). The width (Figure 39, bottom) exhibits an overall increase with time. The varying nature of the width is probably due to local environmental changes.

I. WIDTH VS. TIME

Figure 41 shows a composite plot of the track widths versus time. These widths are much more linear than the earlier plots of the track widths because the widths were averaged for this case. Three features can be extracted from this plot. The first is that the widths generally increase with time. Secondly, the rate or slope of width increase is similar for most of the tracks. However, there are several outliers. The large positive slope to 12 kilometers is ship track 3EJ15 from FIRE depicted in Figure 3. The curved shape of the track in Figure 3 indicates that it passed across wind shifts and probable wind speed changes. These changes may have introduced some errors during the distance-to-time conversion. However, even near the head of the track the slope is somewhat greater than the average of all other tracks. Finally, the track widths that do decrease with time are from ASTEX. This lends itself to the theory that in the Azores there are larger scale circulations that can vary the structure of the tracks more than in the eastern Pacific.

J. DISPERSION VS. DISTANCE FROM SOURCE

The Pasquill-Gifford diagrams, Figure 42, indicate the rate of dispersion expected for over land cases (Dutton and Panofsky, 1984). They are divided into groups of meteorological conditions known as the Pasquill classes. These curves provide a graph of horizontal dispersion as a function of distance from the source. The horizontal dispersion represents the position of maximum visible width.

The diagrams are intended for use over land and smooth terrain. Also, the distance from the source is representative of average times of a few minutes. In this discussion, the ship track cases are obviously over water and represent tracks that are formed over several hours. Therefore, the results do not represent exact meteorological conditions or decay rates. However, they do give us a general indication of the manner in which ship tracks will disperse with time.

For this discussion a neutral, stable and unstable atmosphere are shown for comparison purposes along with the ASTEX and eastern Pacific cases. Figure 42 indicates that the the eastern Pacific cases are less efficient at dispersion over water than they would be over land. The ASTEX tracks disperse more rapidly with distance.

K. DELTA VS. AMBIENT REFLECTANCE

The $\Delta\rho$ versus the ambient reflectance is presented in Figure 43 for all tracks. Generally, as the ambient reflectance increases the environment should be less susceptible to ship effluent and consequently the $\Delta\rho$ should be less. Figure 43 shows that the individual cases have a negative slope indicating that the $\Delta\rho$ does decrease with increasing ambient reflectance. However, in the composite, as

shown by the best fit line, the slope is actually positive. This surprisingly implies that as the ambient reflectance increases, the $\Delta\rho$ also increases and the environment becomes more sensitive to ship effluent. The justification for this may lie in the difference between the boundary layers for the two areas. Atmospheric soundings from the Azores and the eastern Pacific Ocean indicate that the boundary layer is deeper in the Azores than off the west coast of the United States. With this in mind, ambient droplets will spend more time in the Azorean boundary layer so they will be able to grow and coalesce to larger sizes. Consequently, the ambient reflectance in the Azores should generally be less. The same theory applies to the ship track reflectance. The ship effluent will have more time to disperse and grow in the deeper boundary layer. As a result the ship track reflectance will be relatively less. The contrary applies to the eastern Pacific Ocean. With a shallower boundary layer, the ambient droplets cannot grow to as large a size so the ambient reflectance will be relatively higher. The ship effluent in the eastern Pacific Ocean will also spend less time in the boundary layer resulting in a relatively larger ship track reflectance. However, there are not enough cases to confirm this hypothesis.

V. CONCLUSIONS AND RECOMMENDATIONS

The primary focus of this discussion was to analyze the spatial, temporal and radiative characteristics of ship tracks. By examining thirteen cases from two different areas of the world, important differences between the ship tracks and their diffusion properties were studied along with some distinction between the environments of the two different regions.

The results of this analysis were successful in defining the differences and noting the commonalities between the two areas. Specifically, the widths of all the tracks generally increased with time. Also, the rate of increase was generally the same at about 1 km per 150 minutes. However, there were outliers. The cases that showed declining widths were from ASTEX. This is explained by the relatively larger scale circulations that are found near the Azores. These larger scale circulations tend to vary the width more in the Azores than in the eastern Pacific Ocean cases. In a few cases the ASTEX tracks dispersed more efficiently than over land, but the majority of the cases from both ASTEX and the eastern Pacific Ocean generally dispersed less efficiently than over land. There may be several explanations for this. First, there may not have been enough cases or days to make an accurate determination. Other mechanisms may be involved complicating ship track formation and dispersion than originally believed. Also, local effects such as vortices and eddies may affect dispersion properties.

One common result was found in ship and ambient reflectances. In individual cases, when ambient reflectance increased, the $\Delta\rho$ decreased. This implied that on an individual basis, the environment was less sensitive to ship effluent when the ambient reflectance increased. But in the composite of all tracks, as the

ambient reflectance increased the $\Delta\rho$ also increased. This implied that in the composite the environment was more susceptible to ship effluent when the ambient reflectance increased. There is a hypothetical explanation for this although not yet proven. The deeper boundary layer in the Azores translates to relatively lower reflectances for both ambient and ship track. The shallower boundary layer in the eastern Pacific Ocean translates to relatively higher ambient and ship track reflectances. This would account for the positive slope of the $\Delta\rho$ versus ambient curve.

The ship track phenomenon can continue to be studied from a variety of approaches. Some of the more prominent include:

--More Ships of Opportunity need to be utilized. By analyzing the fuel of known ship track makers, and the plume in the contaminated cloud, a study can be performed examining the changes the exhaust undergoes.

--The possibility of a more automated and accurate manner of determining track width needs to be further explored. Many of the uncertainities are produced as a result of the subjective methods used to determine track width.

--The meteorological conditions associated with a ship track must be accurately identified, especially the true wind. This is crucial in determining the relative wind and matching the track with the correct ship. Also, any local effects need to be identified along with synoptic features i.e. fronts.

--The role of vortices, turbulence and dispersion must be studied further. These properties of the atmosphere will help to explain the physical structure of ship tracks and their decay with time.

This work has proveded initial results for spatial and radiative characteristics of ship tracks. It is now important to more fully explore the recommendations

discussed above. A concerted effort in these areas will yield relevant information which can then be consolidated to understand and forecast ship track formation.

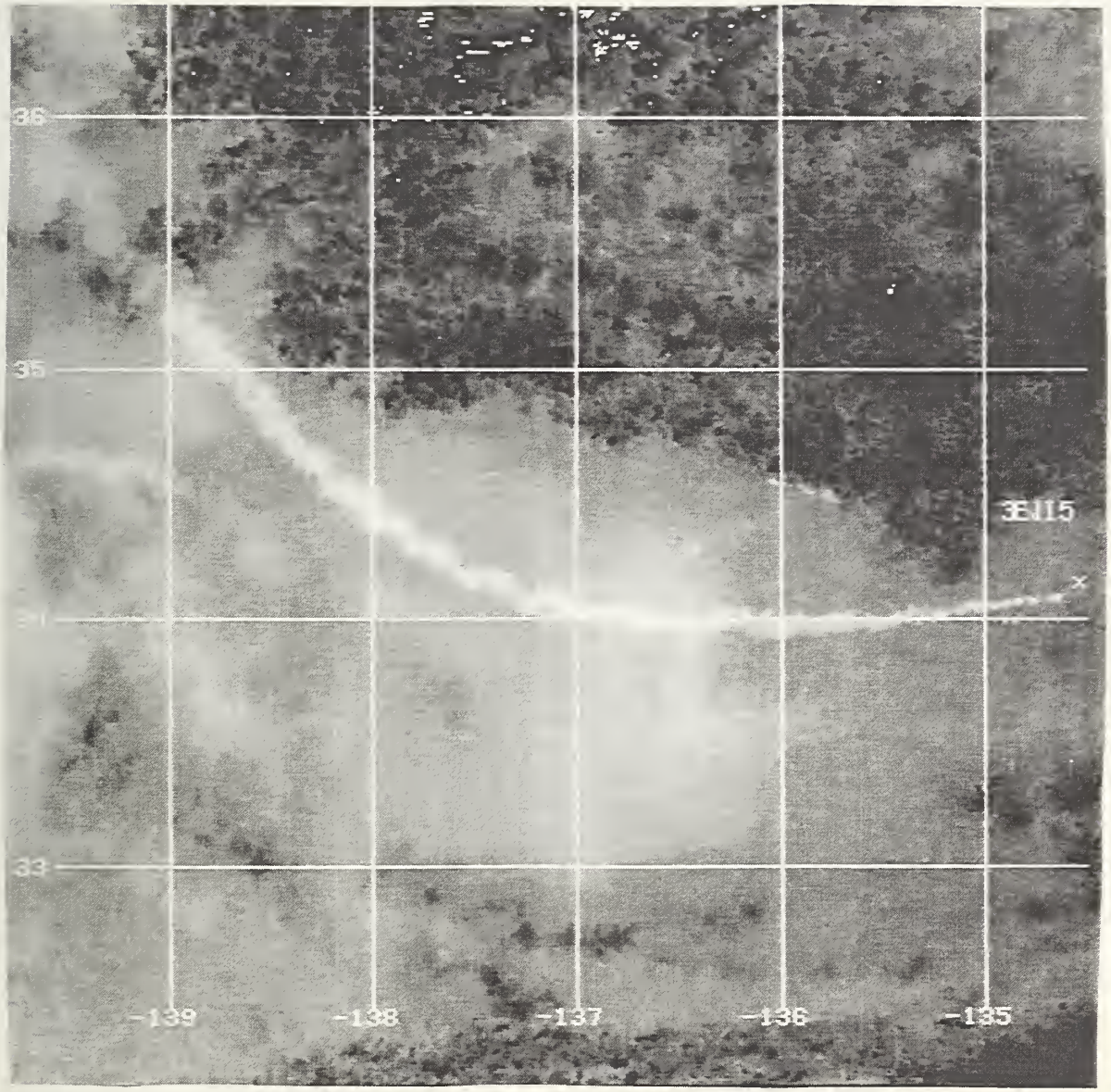

Figure 3. NOAA-10 1639Z 7 July 1987 (Channel 2)

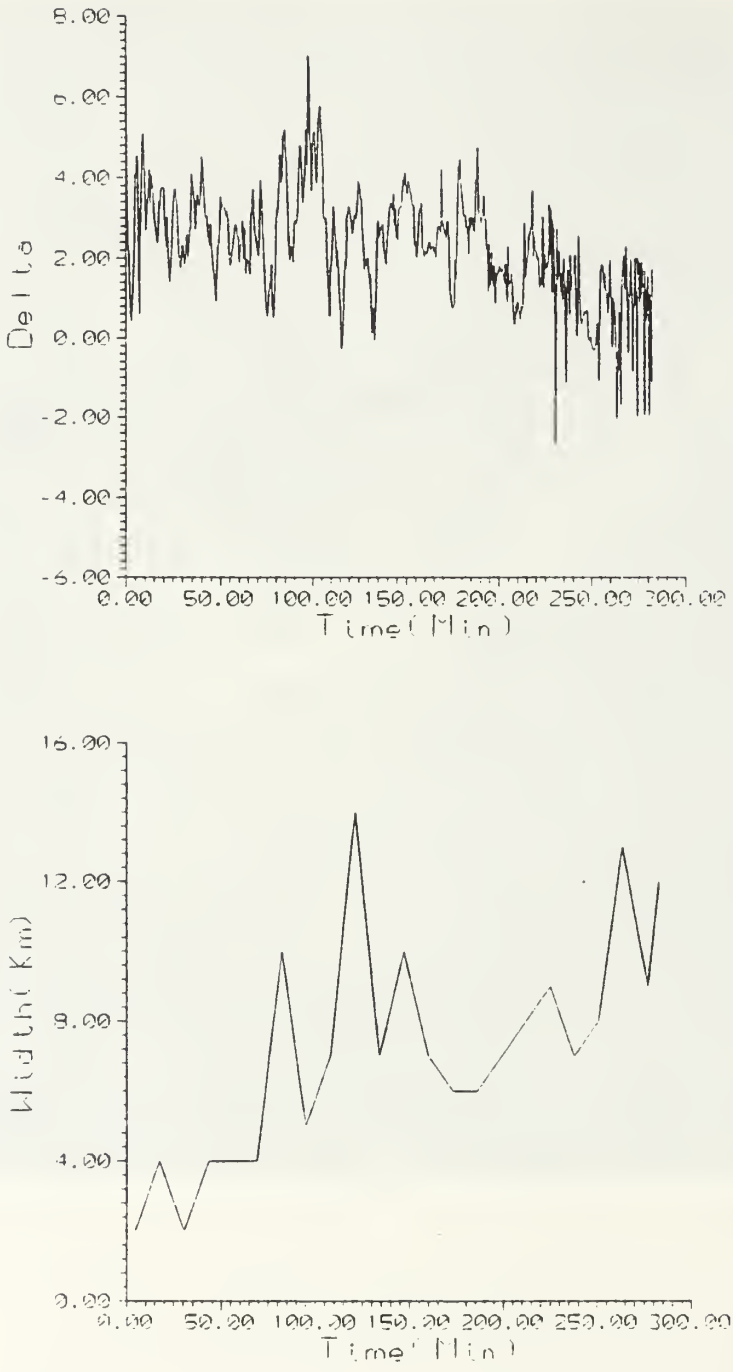

Figure. 4. NOAA-10 1639Z 7 July 1987 Delta Ch.3 Temp and Track width(Bottom).

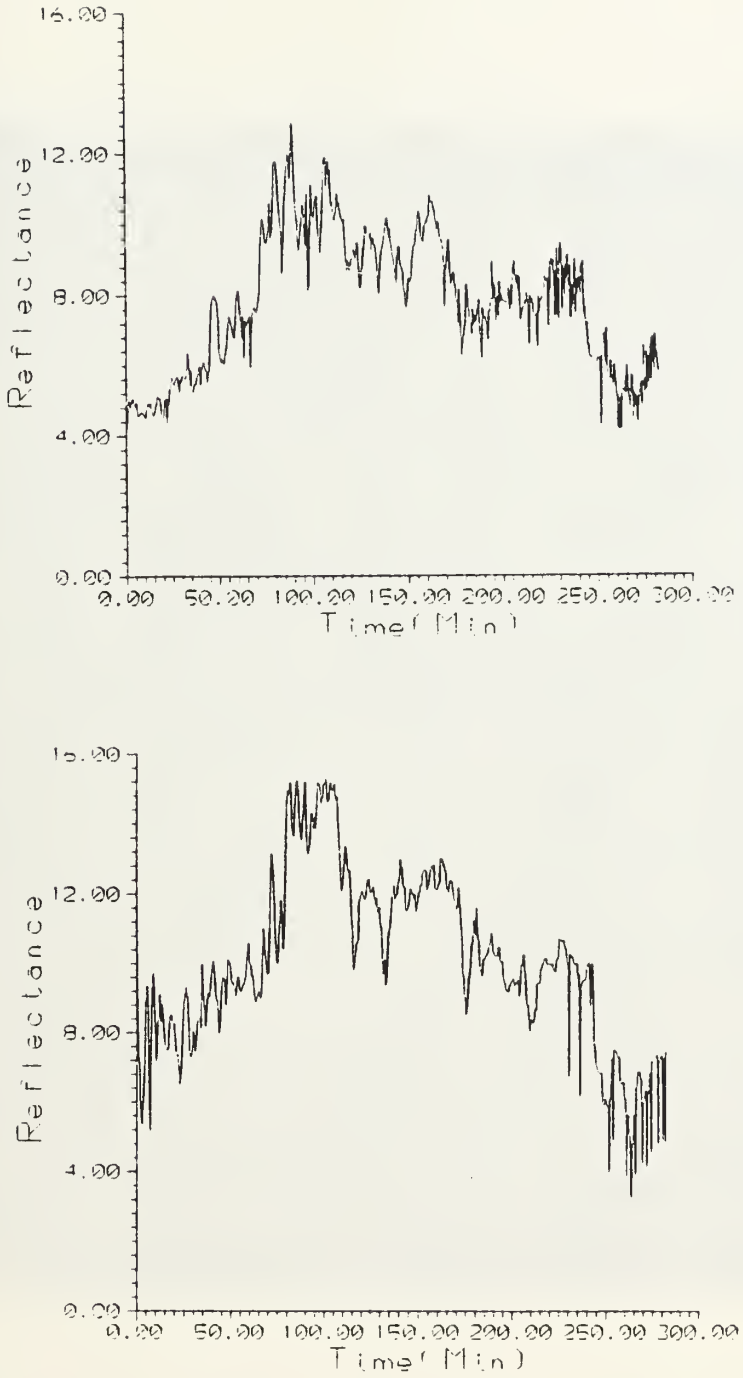

Figure 5. NOAA-10 16307 7 July 1987 Ambient Ch 3(Top) and ship track Ch 3(Bottom)

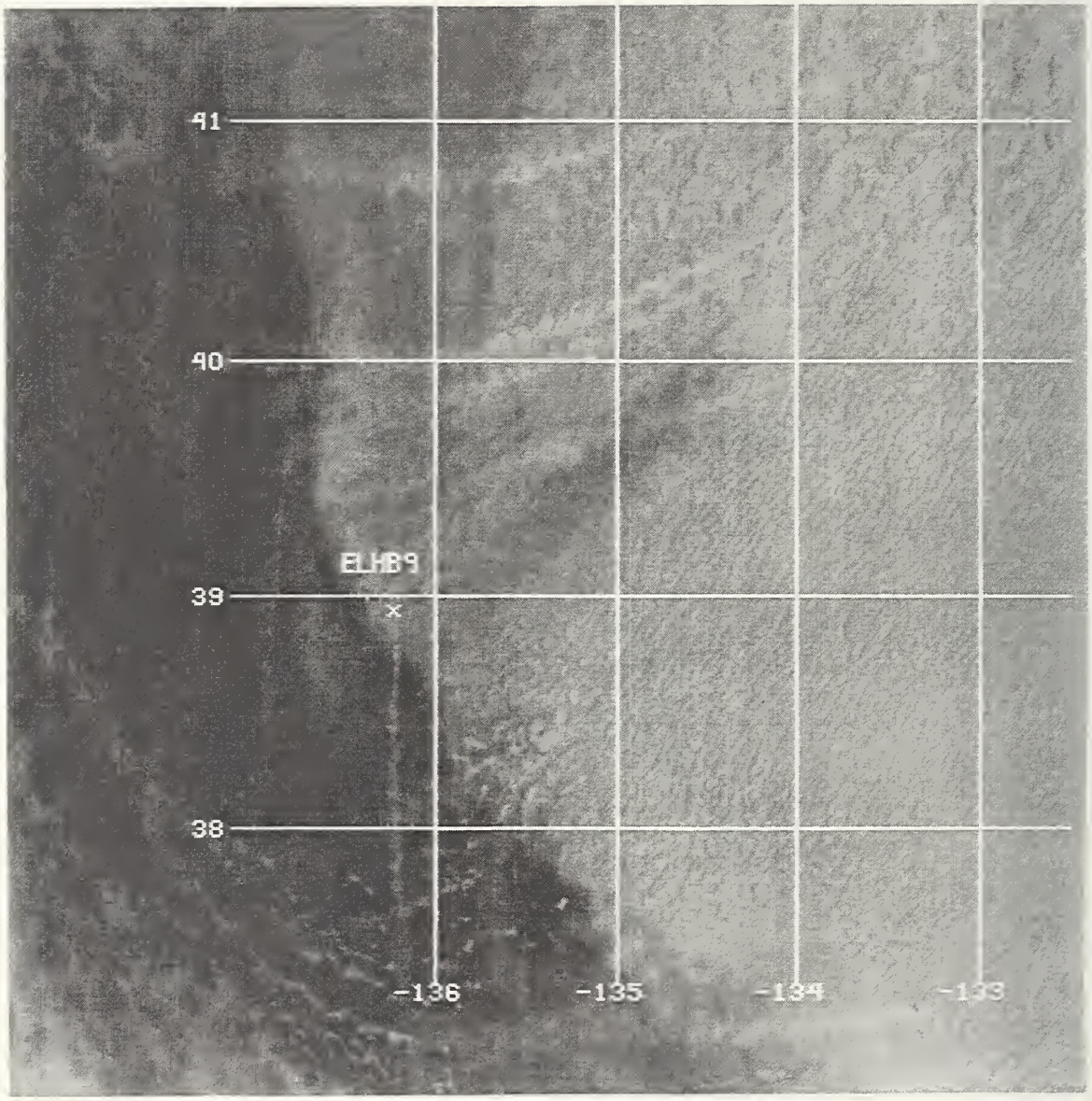

Figure 9. NOAA-9 2303Z 14 July 1987 Ch.3.

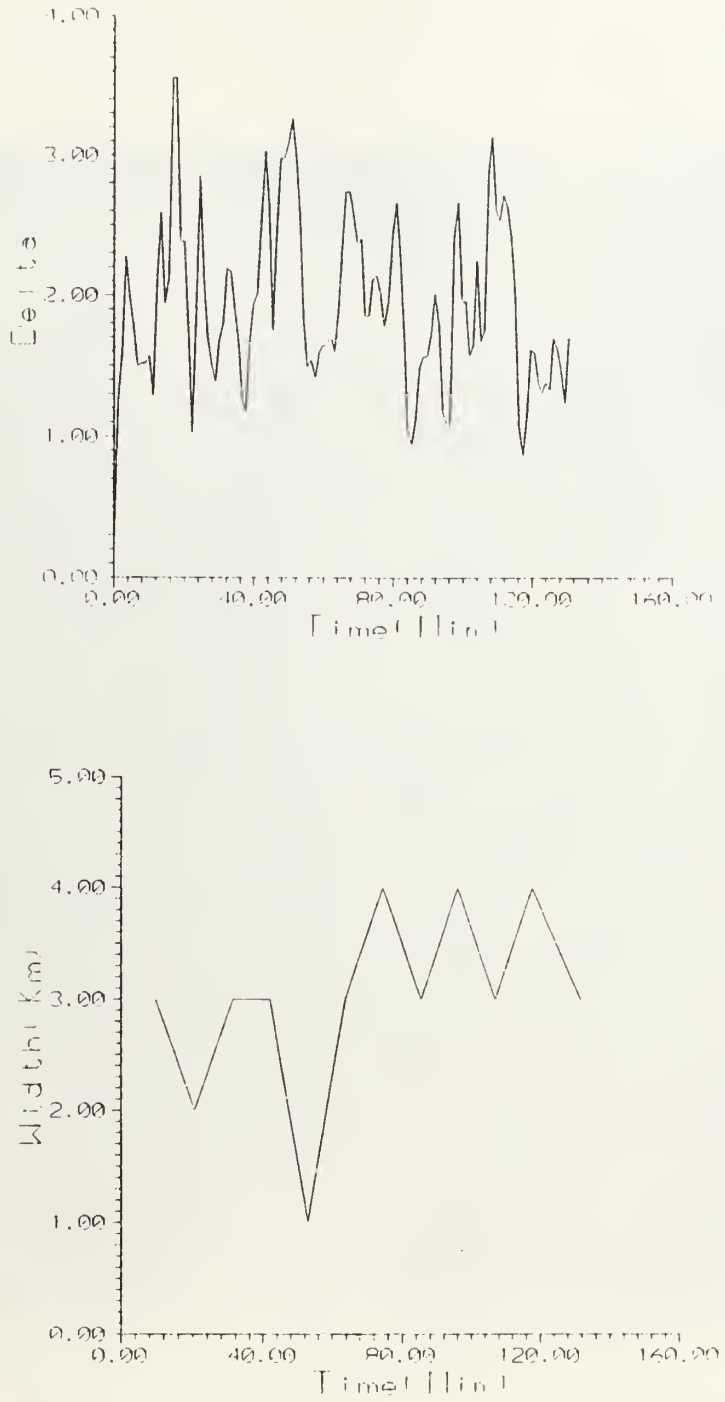

Figure 7. NOAA-9 23037 11 July 1987 Delta Ch.3(Top) and Track width(Bottom).

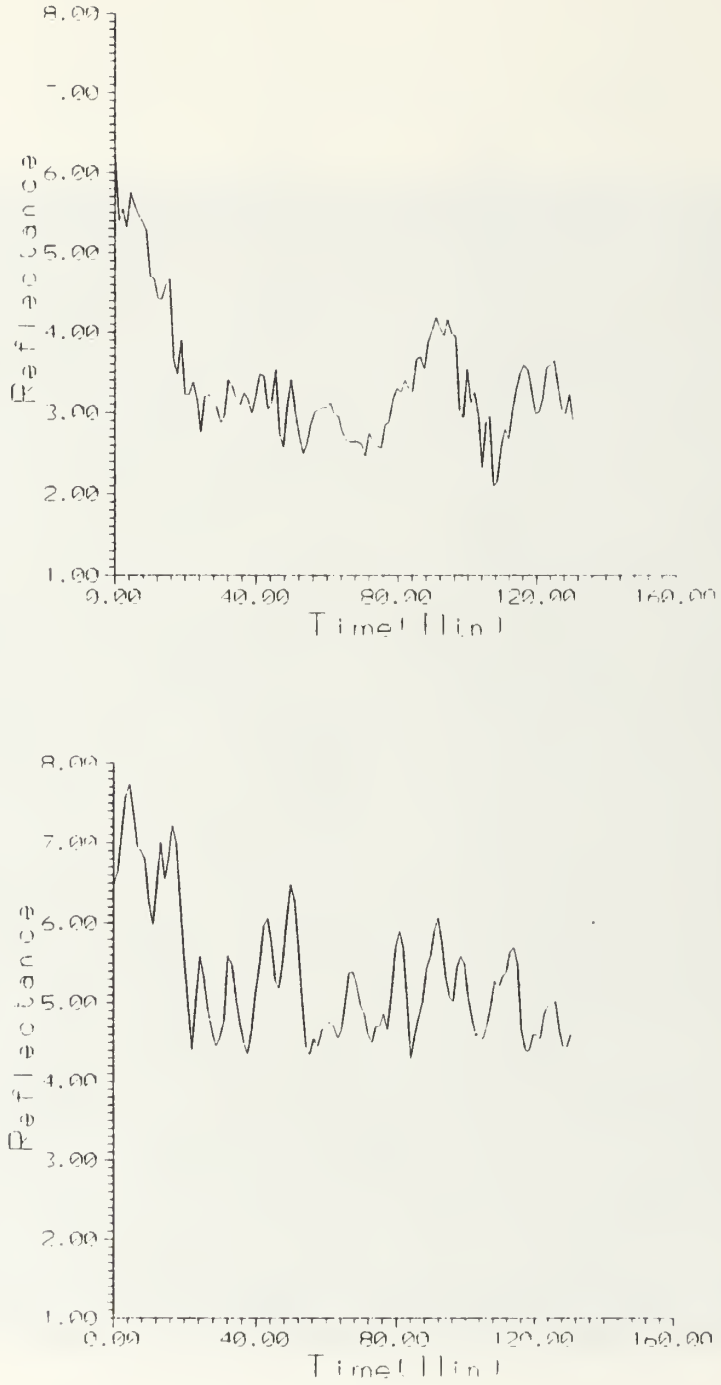

Figure 8. NOAA-9 2303Z 14 July 1987 Ambient Ch.3(Top) and Ship track Ch.3(Bottom).

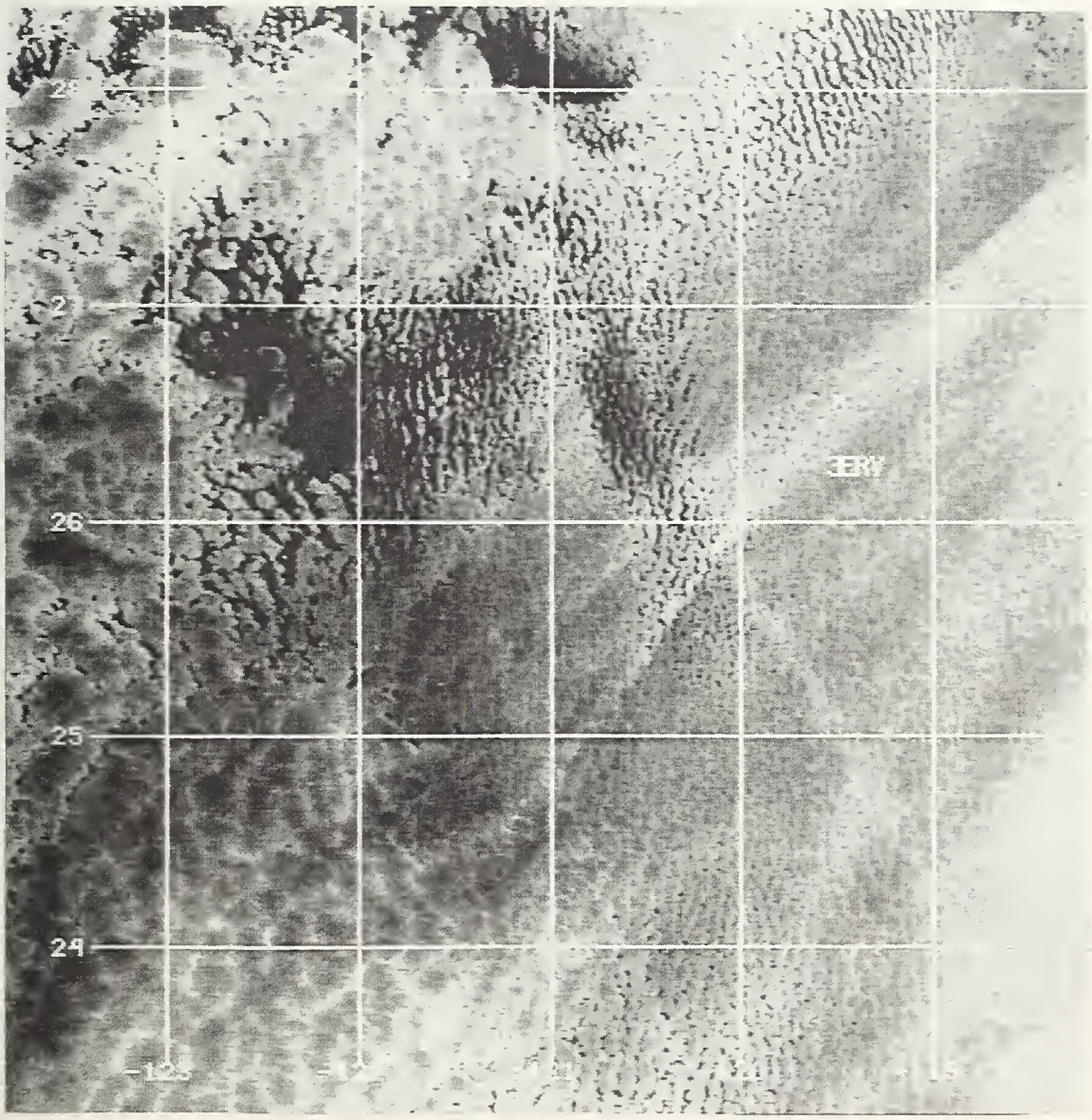

Figure 9. NOAA-10 1604Z 4 July 1987 Ch.3.

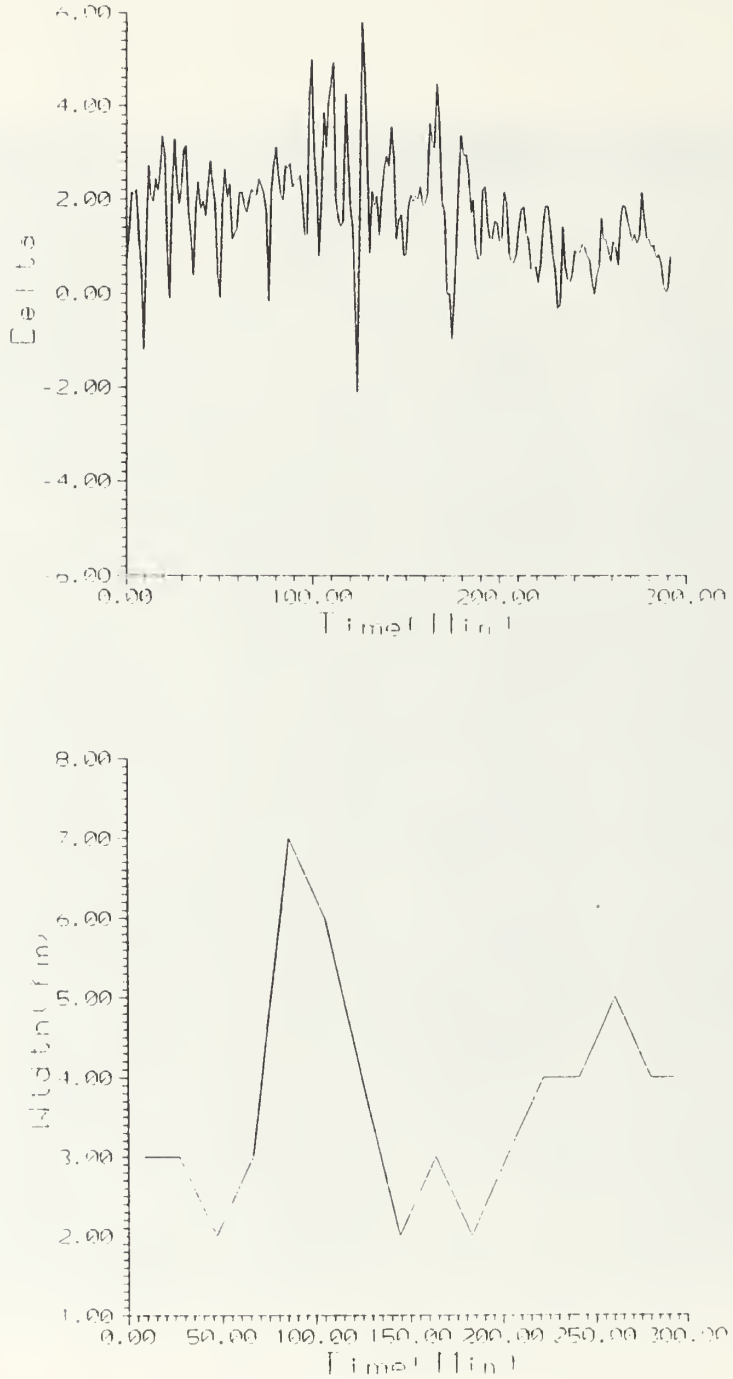

Figure 10. NOAA 10 16017 (July 1987 Delta Ch.3 (top) and Track width(Bottom).

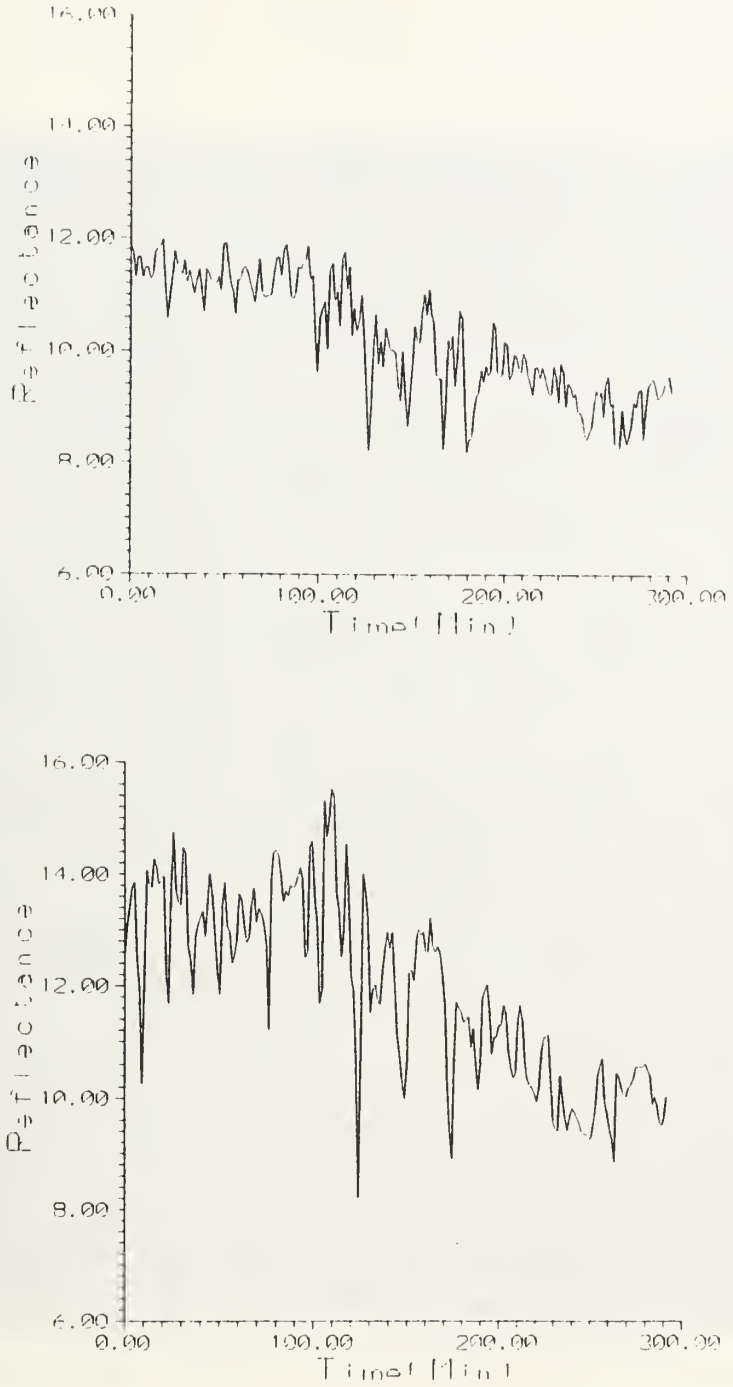

Figure 11. NOAA-10 1601Z 4 July 1987 Ambient Ch 3(Top) and Ship track Ch 3(Bottom).

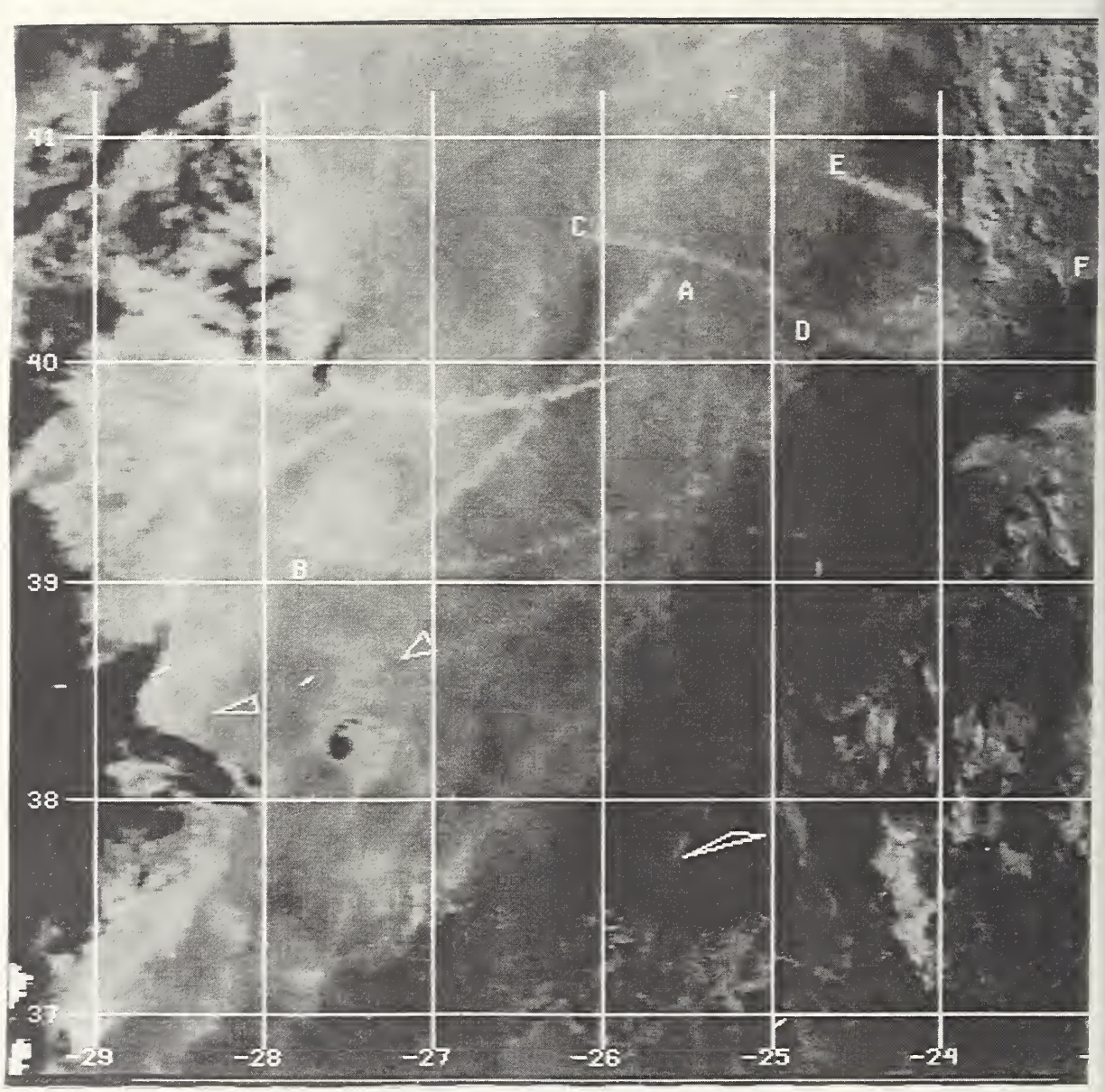

Figure 12. NOAA-12 0903Z 14 June 1992 Ch.3.

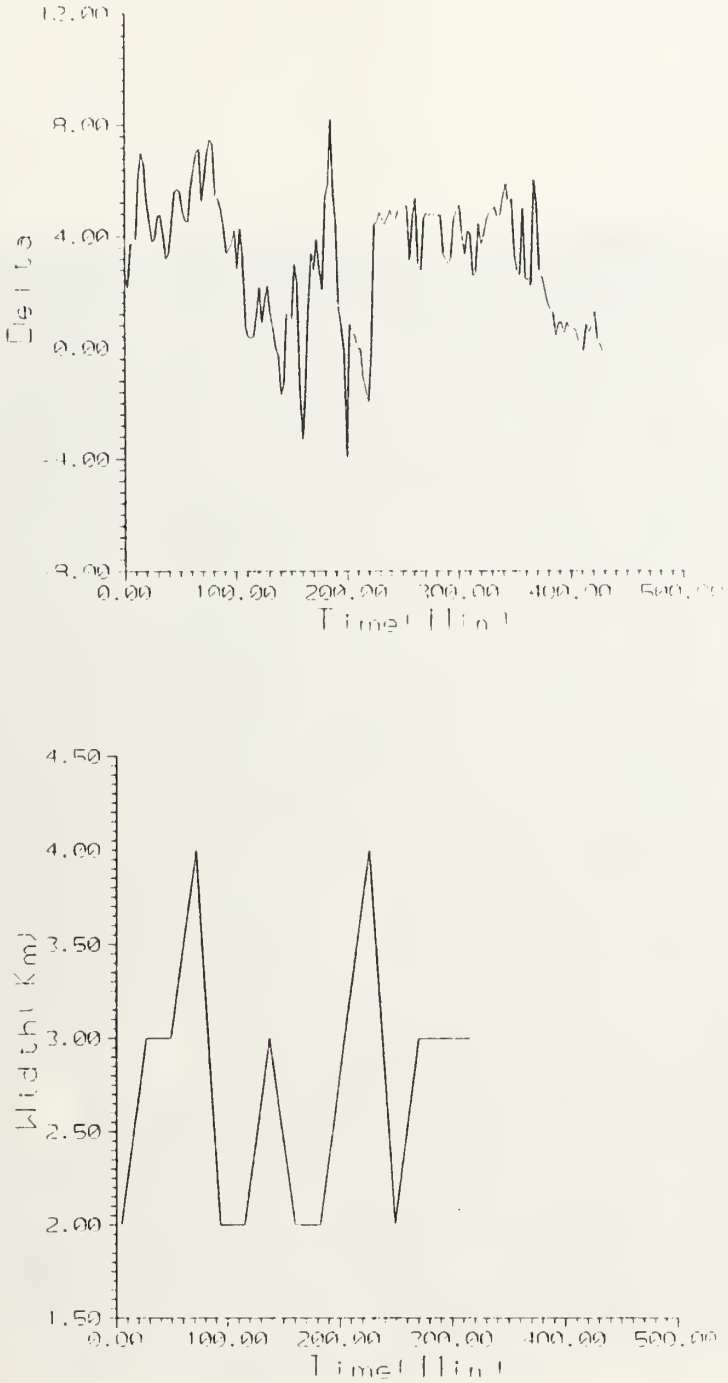

Figure 13. NOAA-12 0903Z, 11 June 1992 Track AB Delta C h 3 (Top) and Track width(Bottom).

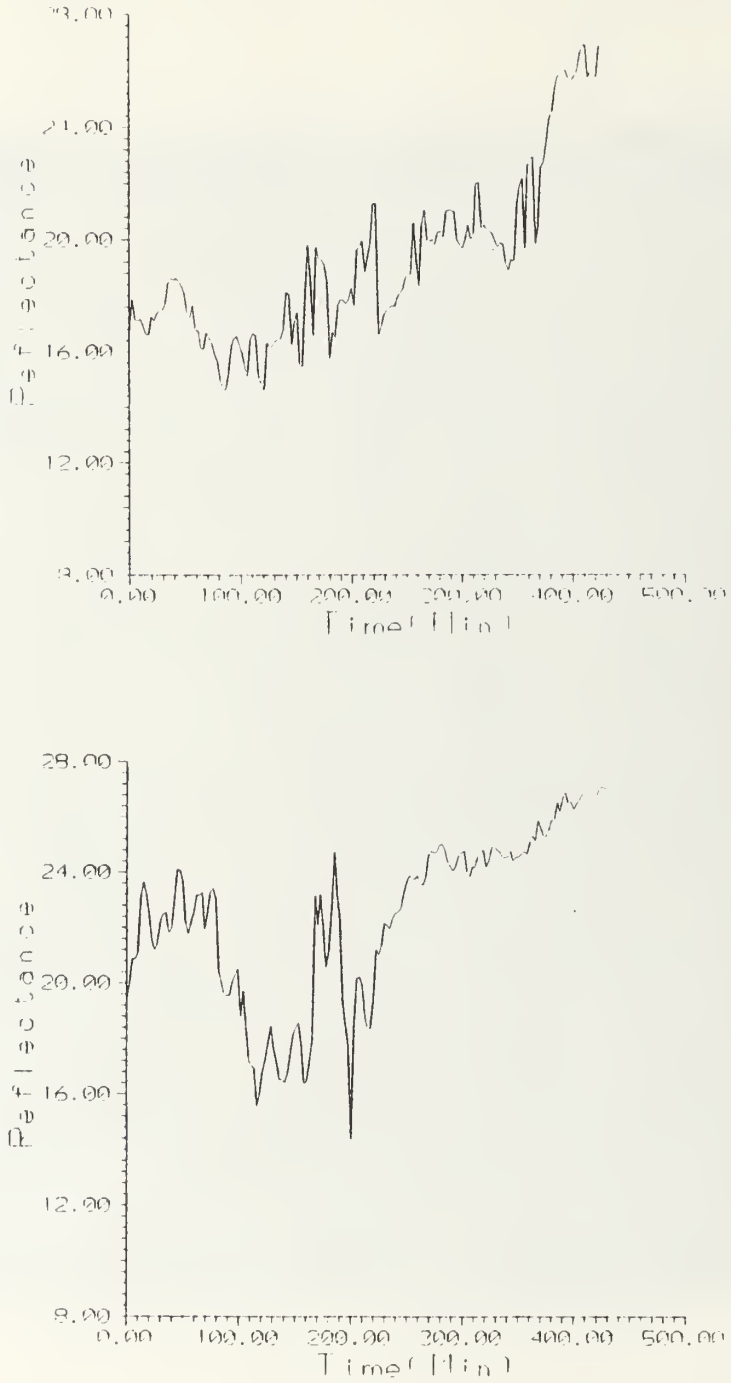

Figure 11. NOAA-12 0903Z, 14 June 1992 Track AB Ambient Ch.3(Top) and Ship-track Ch.3(Bottom).

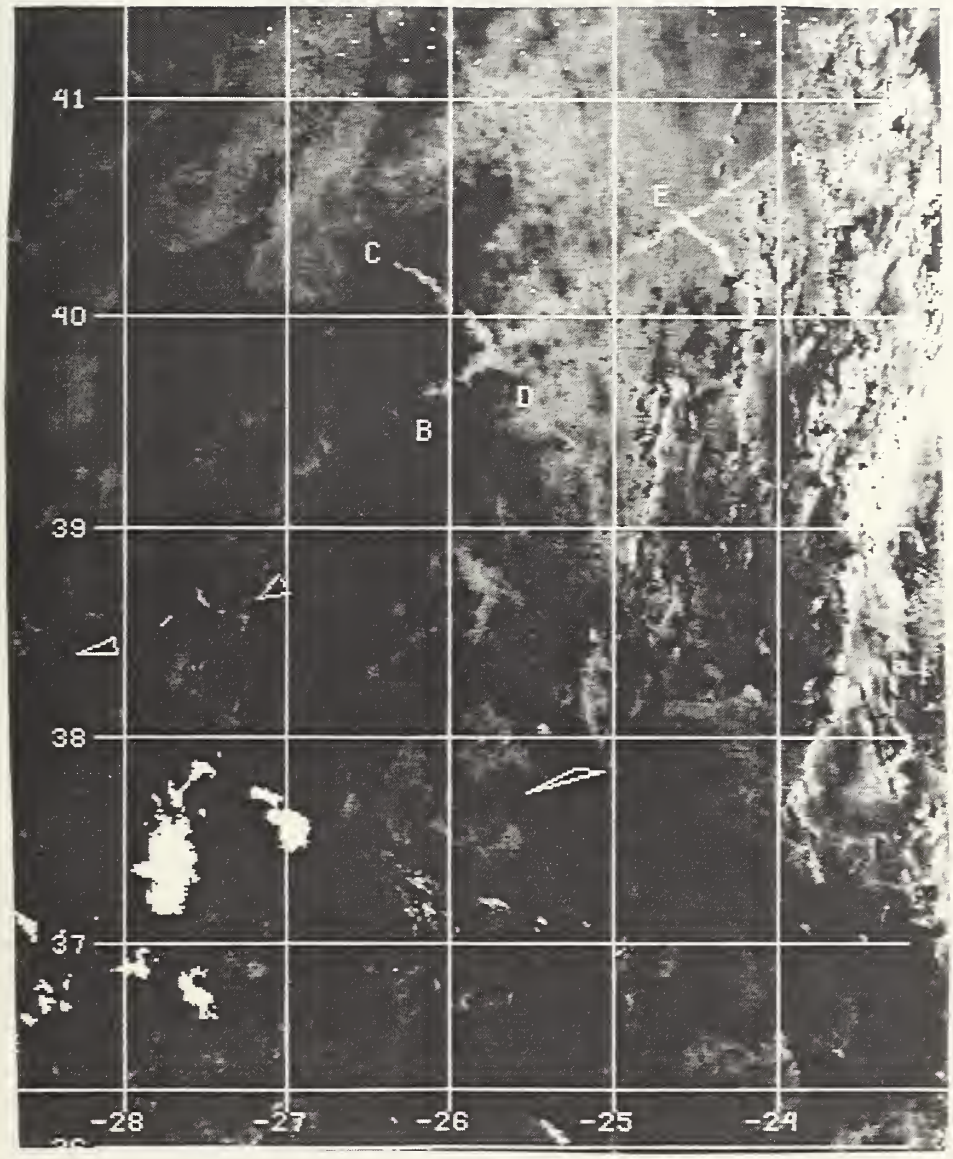

Figure 15. NOAA-11 1625Z 14 June 1992 Track AB Ch.3.

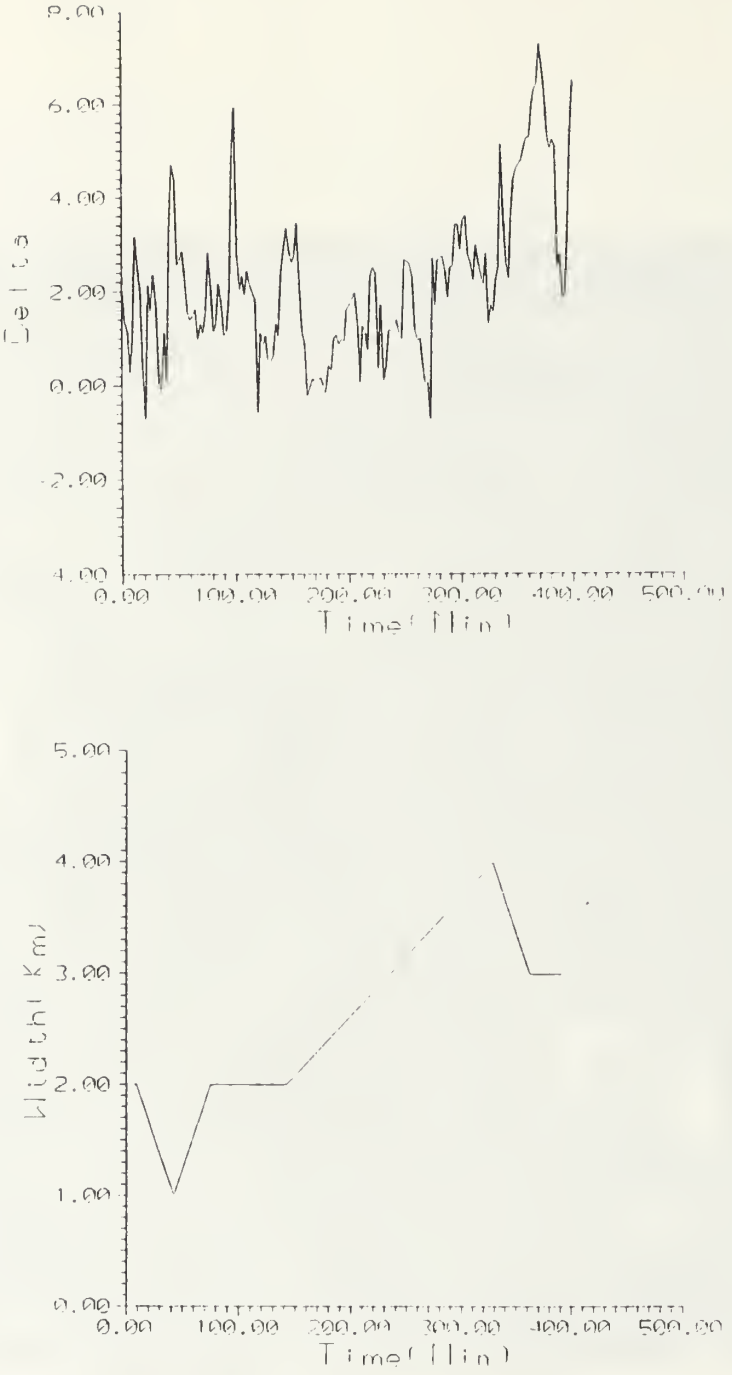

Figure 16. NOAA 11 1625Z 11 June 1992 Track AB Delta Ch.3(Top) and track width(Bottom)

Figure 17. NOAA-11 1625Z 11 June 1992 Track AB Ambient Ch.3(Top) and Ship-track Ch.3(Bottom).

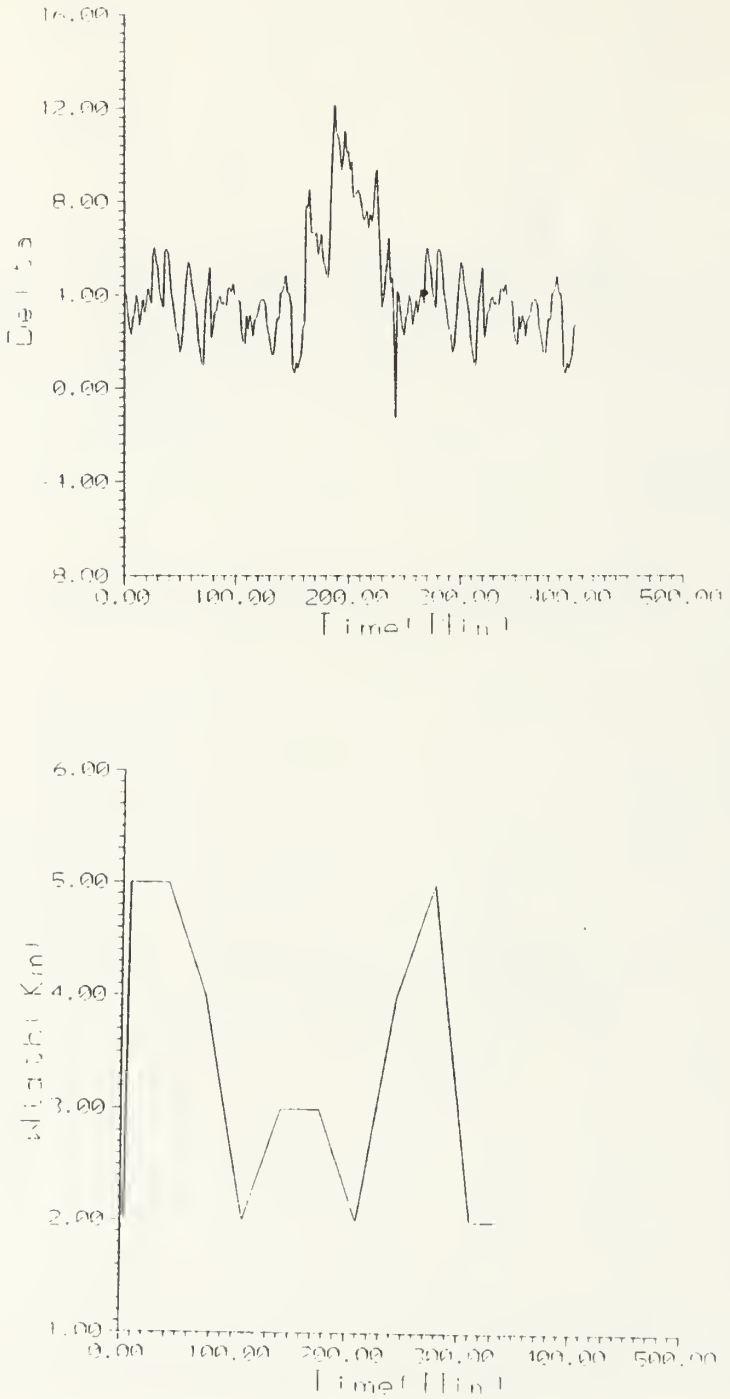

Figure 18. NOAA 12 0903Z 11 June 1992 Track C D Delta Ch 3 Temp and Track width(Bottom).

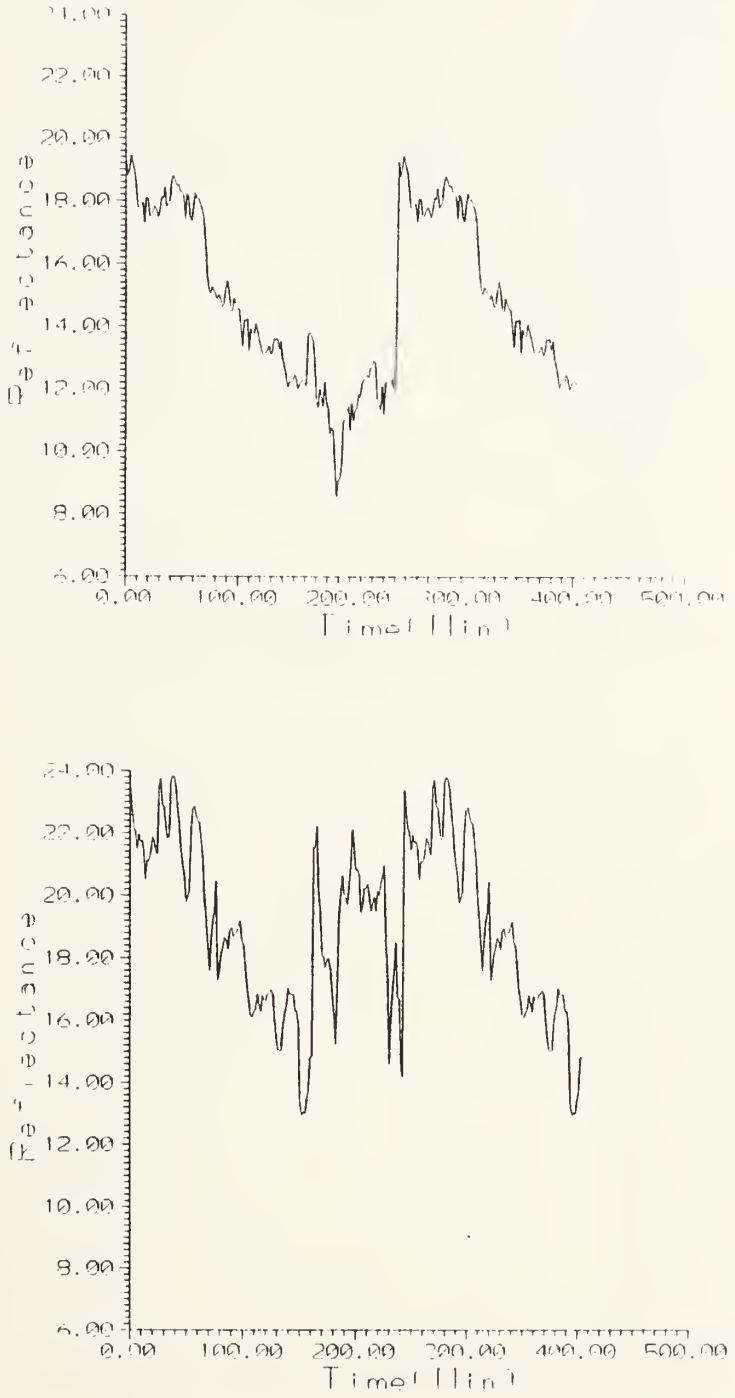

Figure 19. NOAA 12 0903Z 14 June 1992 Track CD Ambient Ch 3(Top) and Ship track Ch.3(Bottom).

Figure 20. NOAA-11 1625Z 14 June 1992 Track CD Delta Ch 3(Top) and Track width(Bottom).

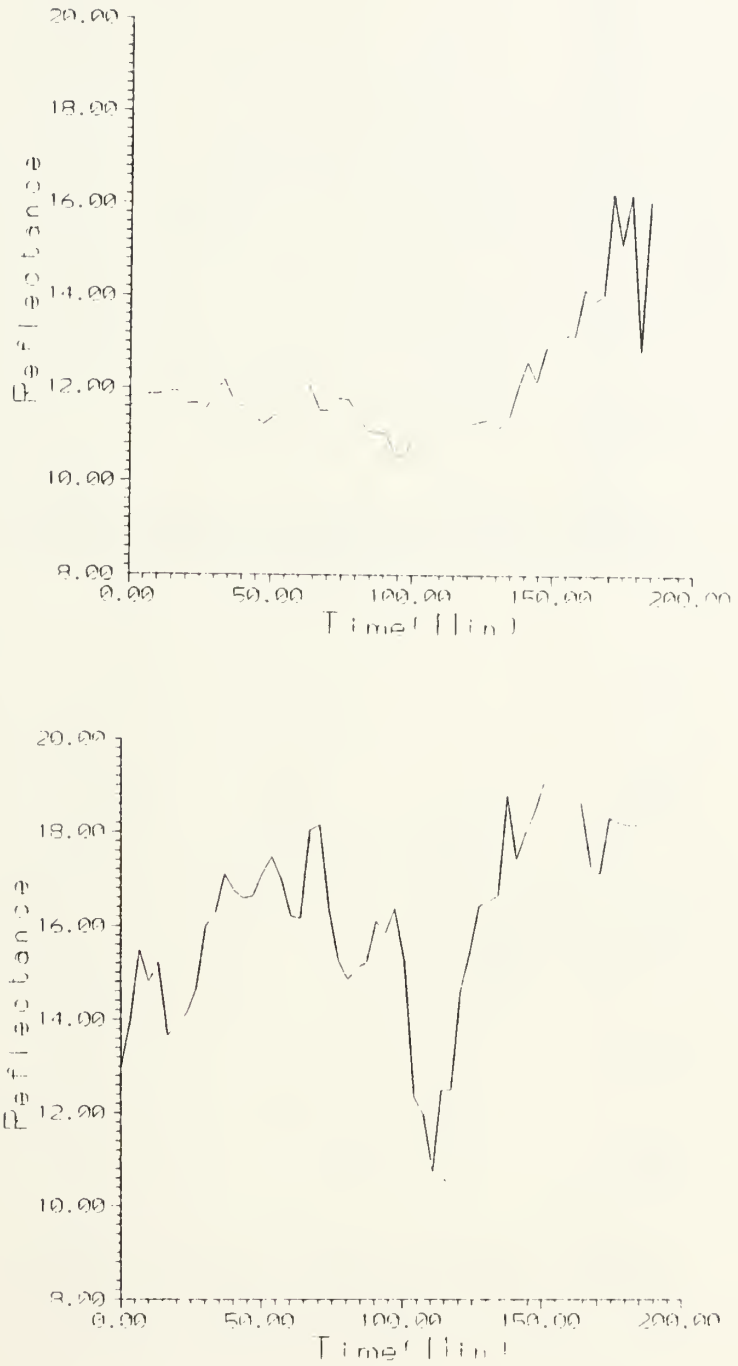

Figure 21. NOAA-11 1625Z 14 June 1992 Track C D Ambient Ch 3(Top) and Ship track Ch. 3(Bottom).

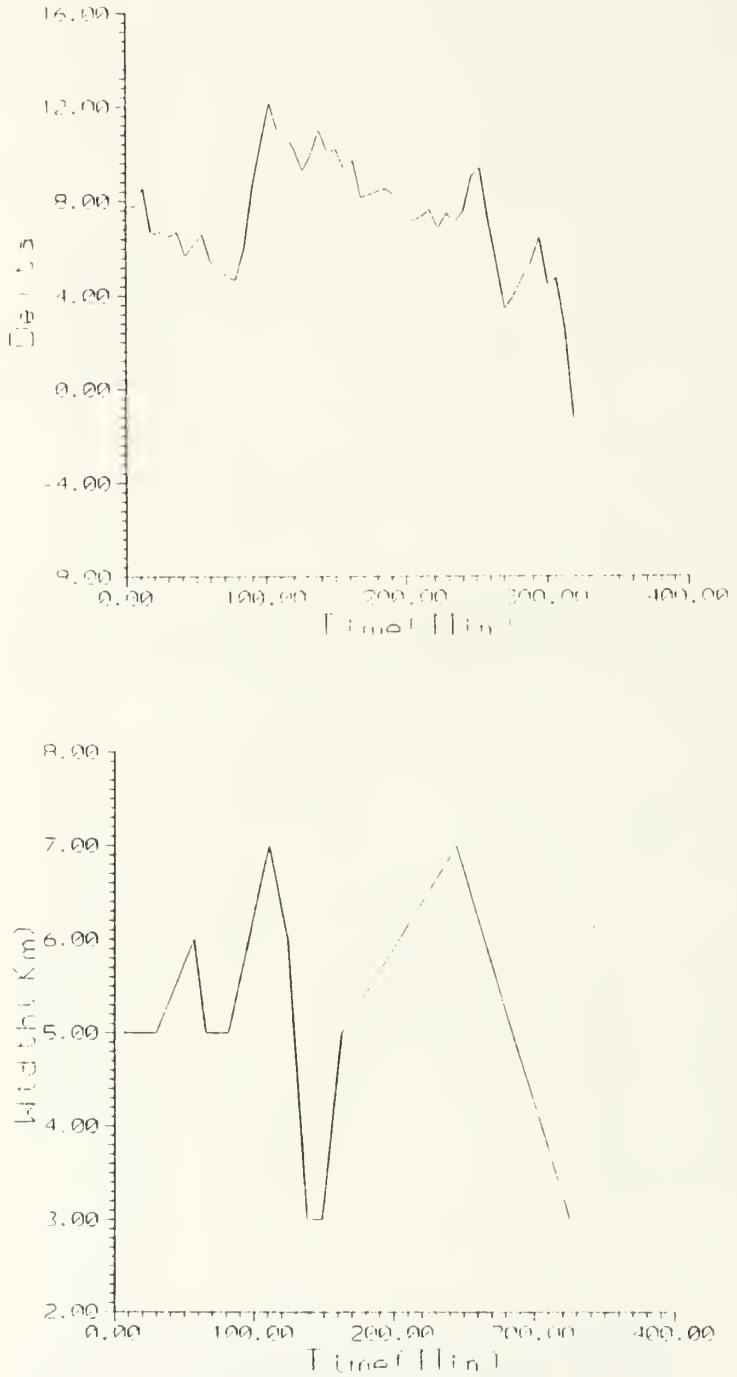

Figure 22. NOAA 12 09037 11 June 1992 Track 11 Delta Ch.3(Top) and Track width(Bottom).

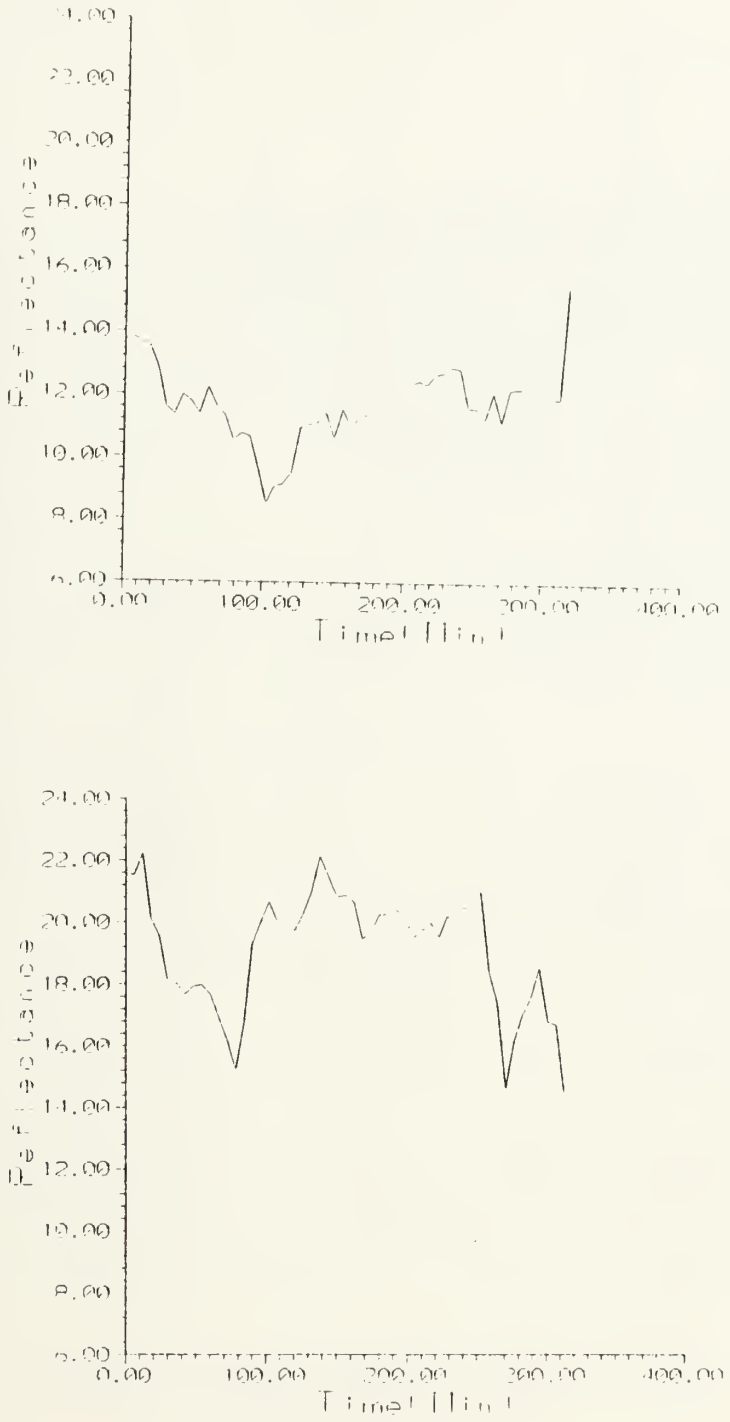

Figure 23. NOAA-12 09037 14 June 1992 Track DE Ambient Ch.3(Top) and Ship track Ch.3(Bottom).

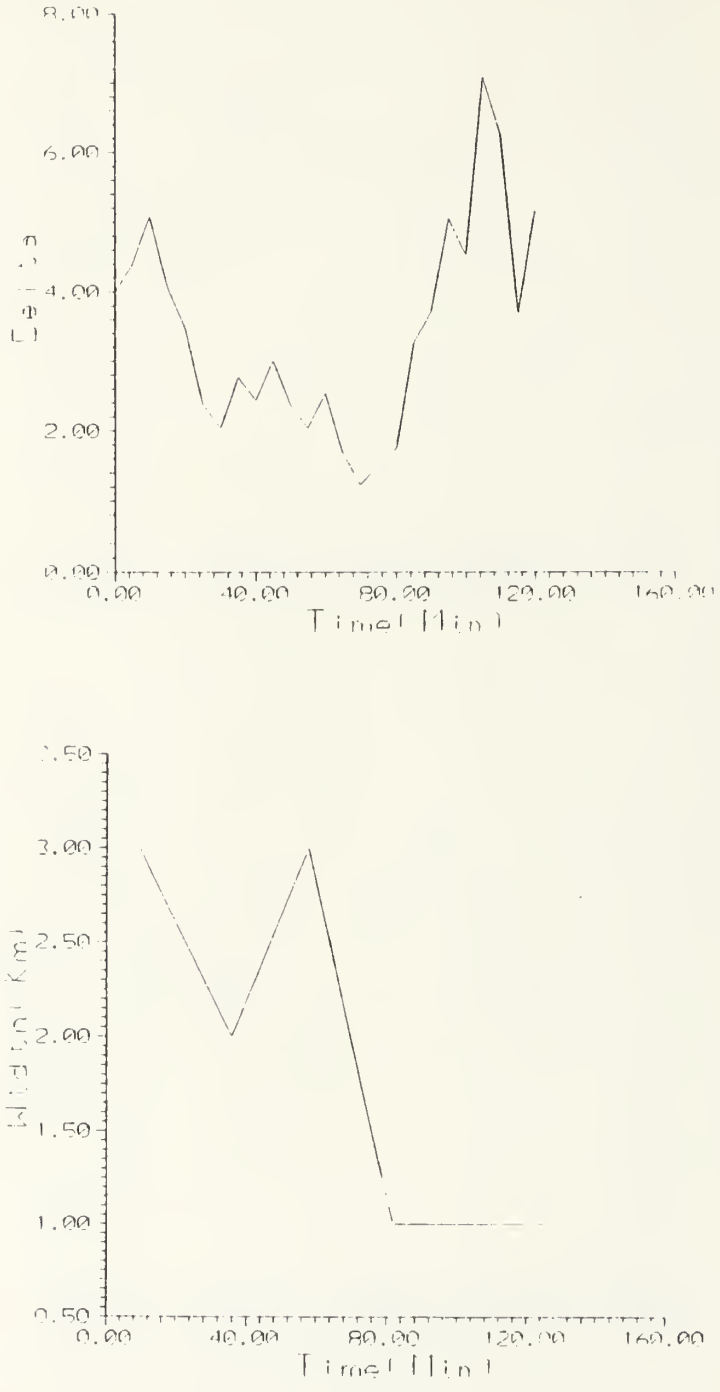

Figure 21. NOAA-11 1625Z 11 June 1992 Track 11 Delta Ch.3(Top) and Track width(Bottom).

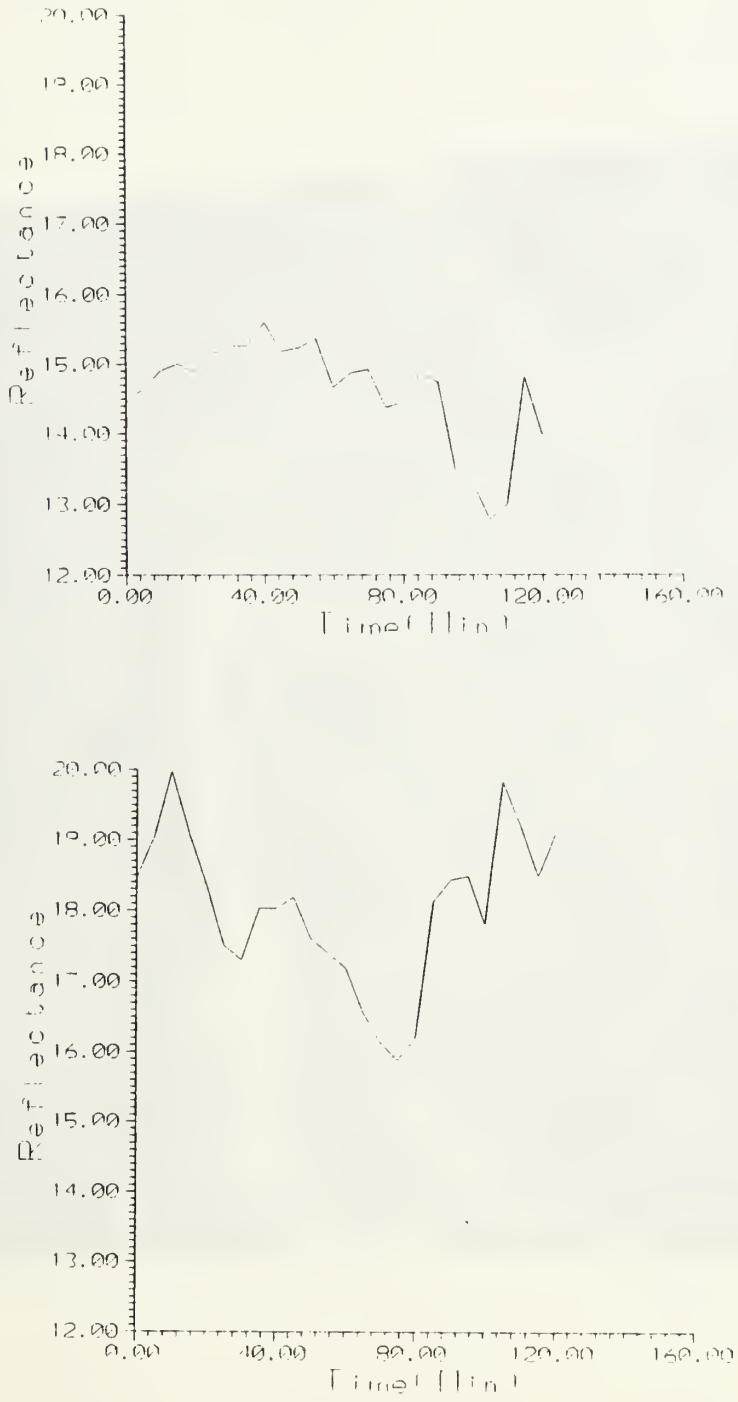

Figure 25. NOAA-11 16257 11 June 1992 Track UF Ambient Ch.3(Top) and Ship track Ch.3(Bottom).

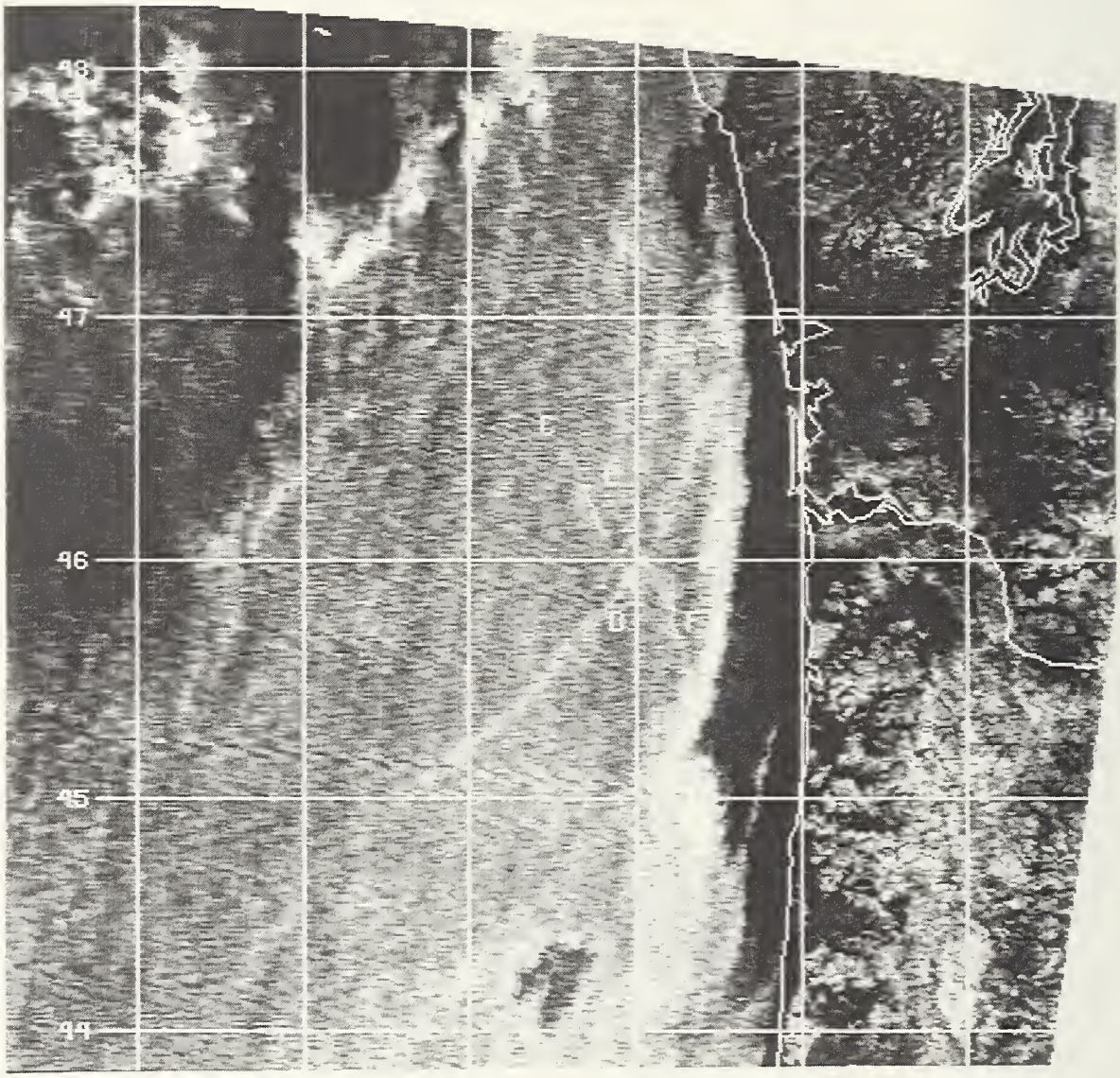

Figure 26. NOAA-10 1510Z 26 August 1992 Ch.3.

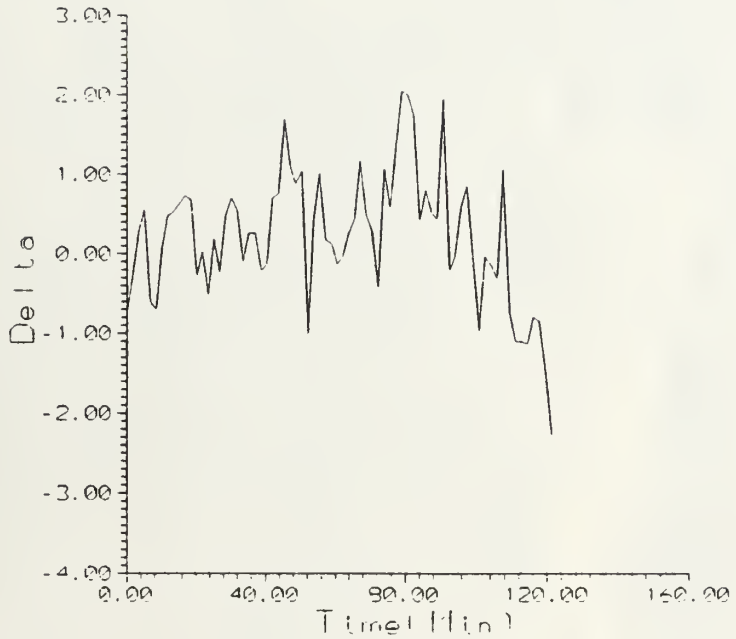

Figure 27. NOAA 10 1510Z 26 August 1992 Track CPD Delta Ch.3.

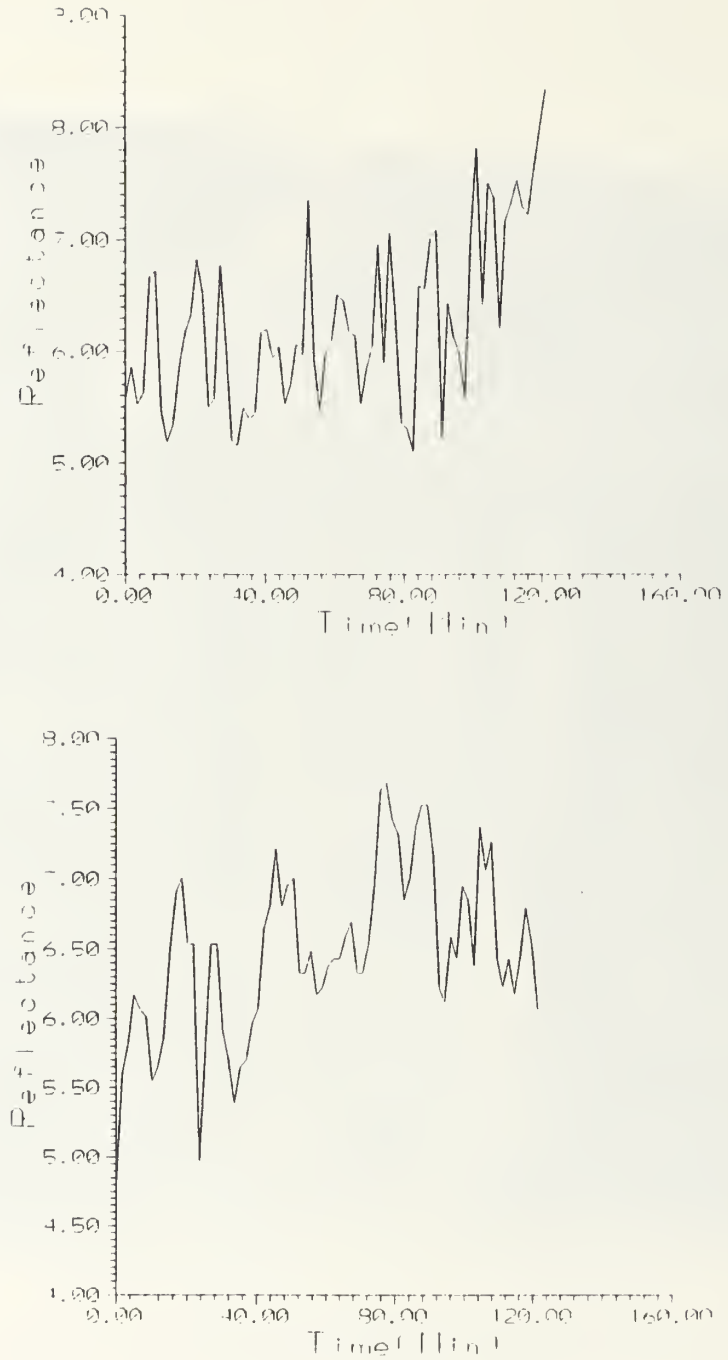

Figure 28. NOAA-10 1510Z 26 August 1992 Track CD Ambient Ch.3(Top) and Ship-track Ch.3(Bottom).

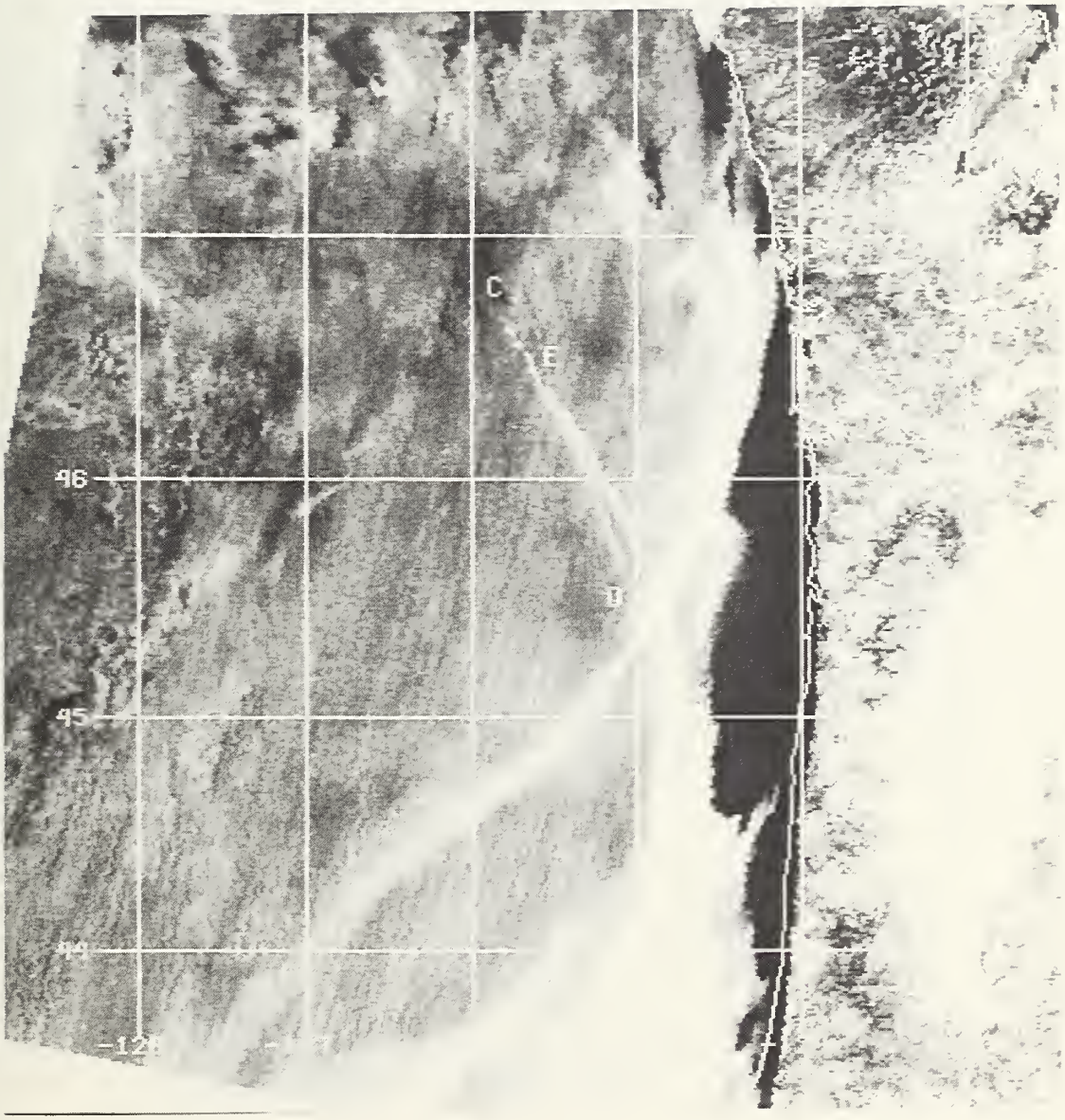

Figure 29. NOAA-12 1635Z 26 August 1992 Ch.3.

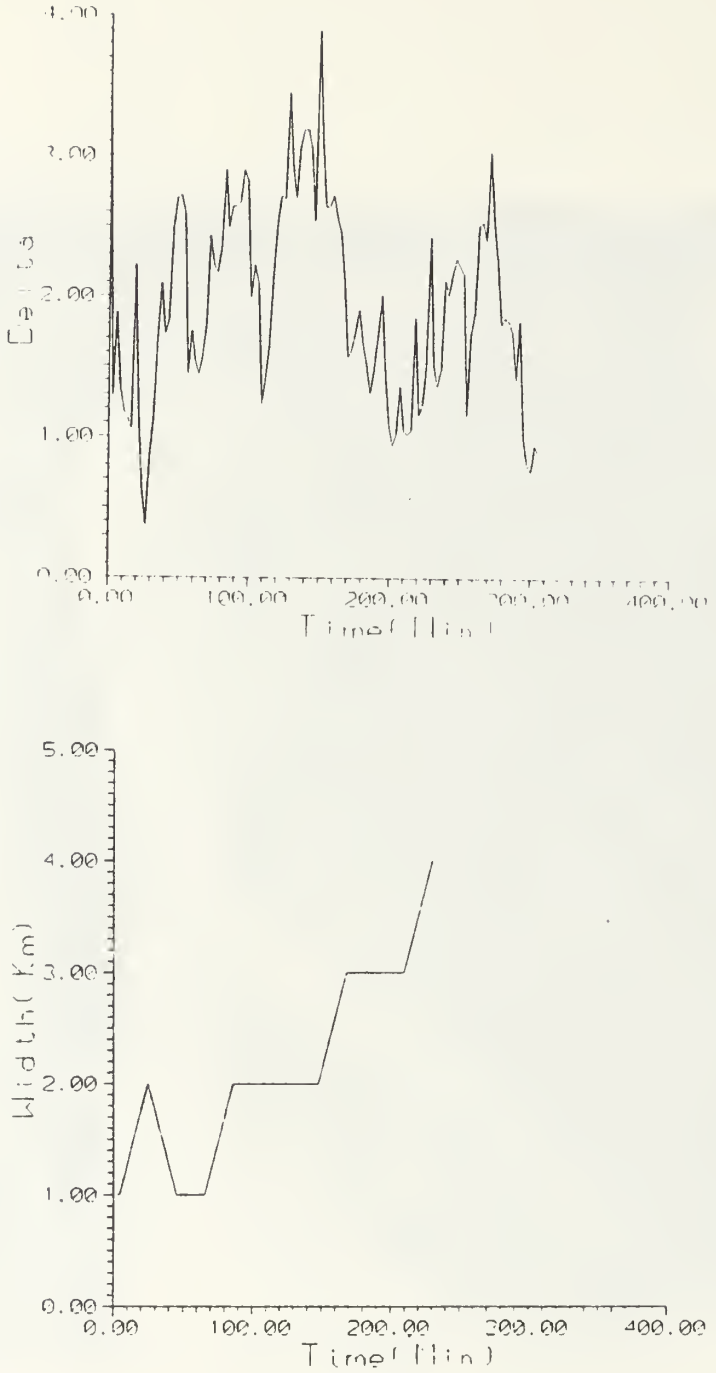

Figure 30. NOAA-12 1635Z 26 August 1992 Track CD Delta Ch.3(Top) and Ship track Ch.3(Bottom).

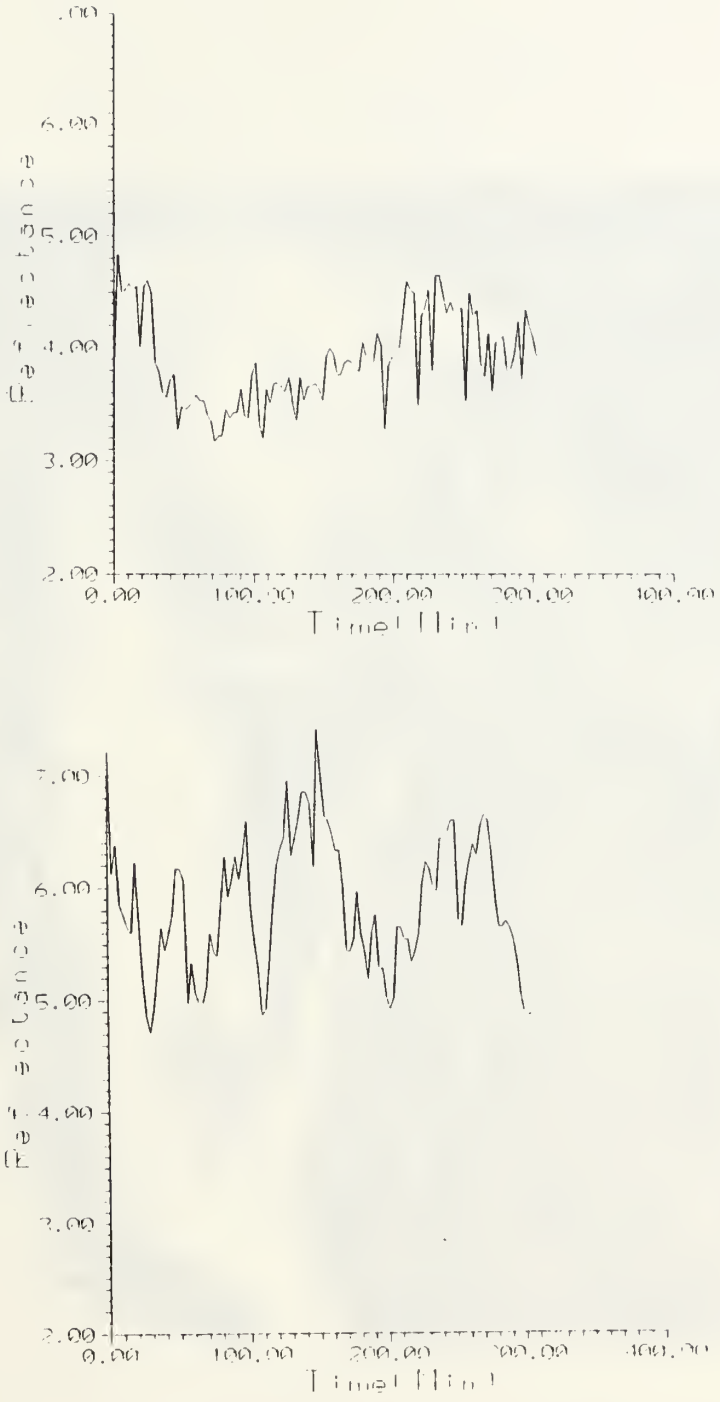

Figure 31 NOAA 12 16357 26 August 1992 Track CD Ambient Ch.3(Top) and Ship track Ch.3(Bottom).

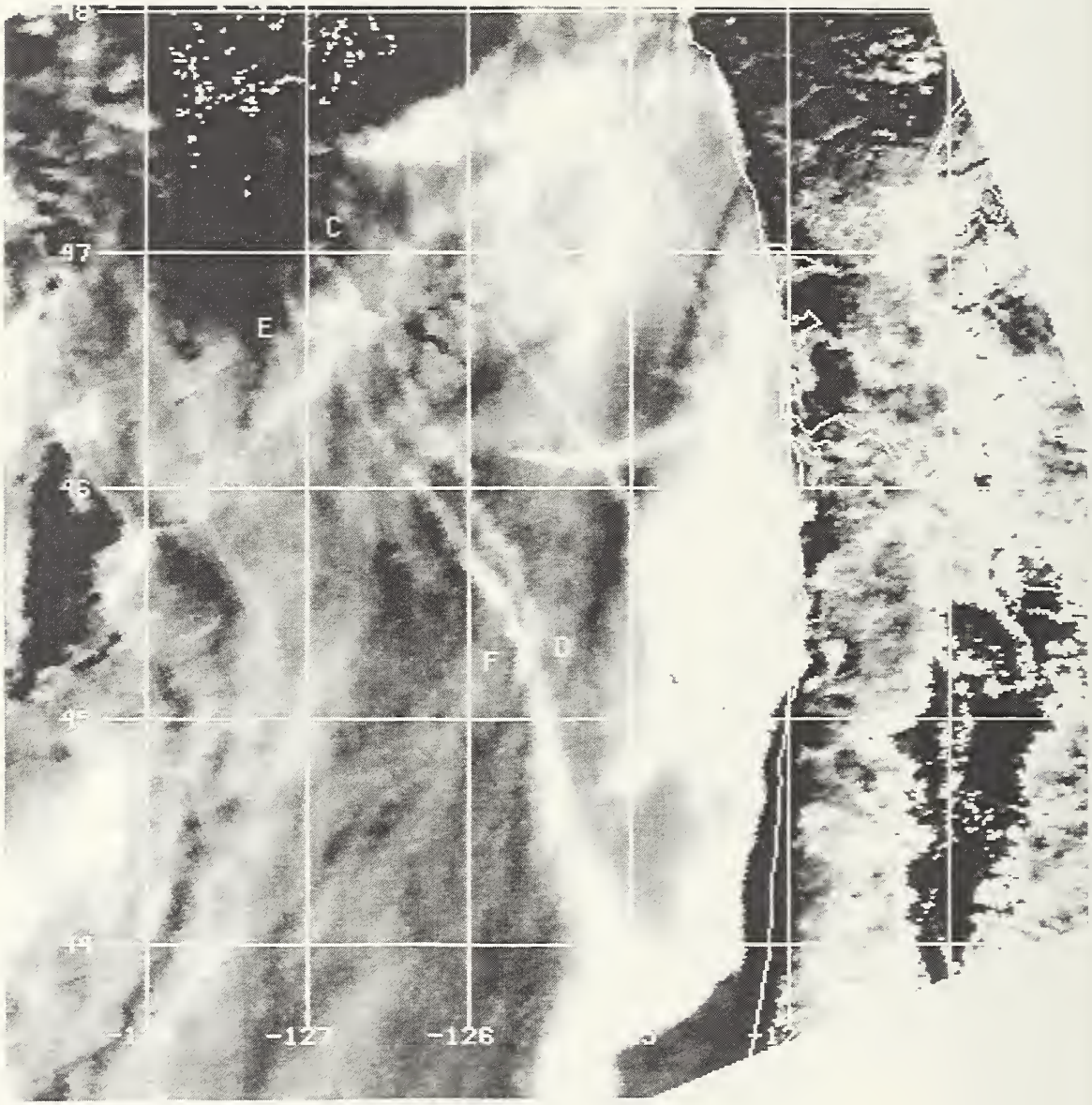

Figure 32. NOAA-11 2204Z 26 August 1992 Ch.3.

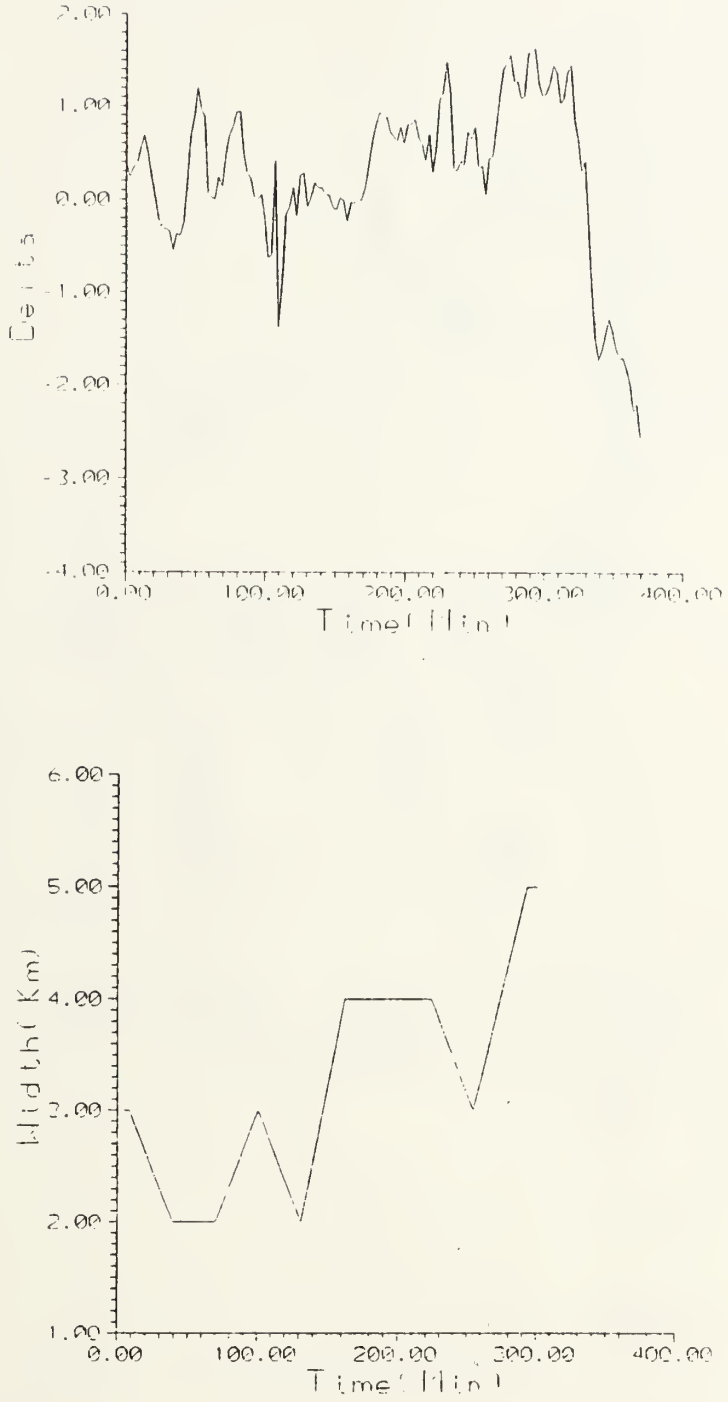

Figure 33. NOAA-11 2201Z 26 August 1992 Track (D Delta (b,3(Top) and Track width(Bottom).

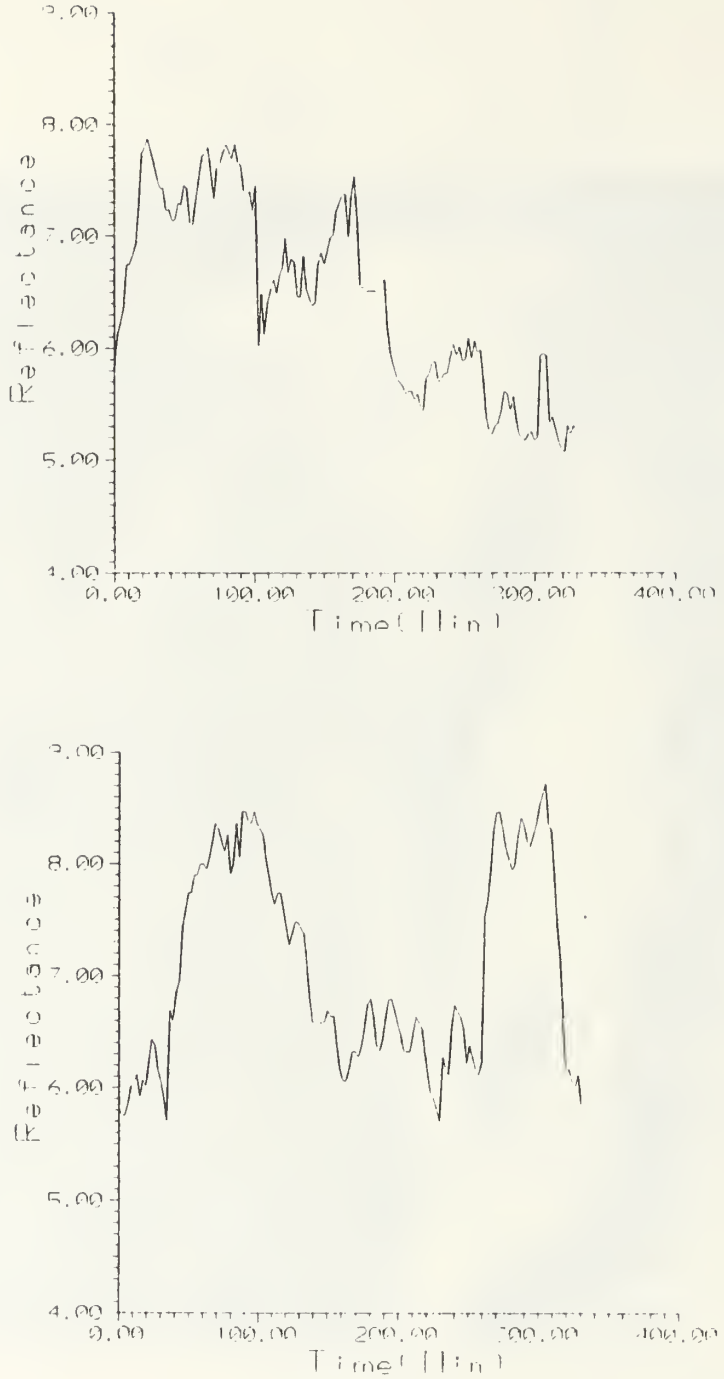

Figure 31. NOAA-11 2201Z 26 August 1992 Track CD Ambient Ch.3(Top) and Ship track Ch.3(Bottom).

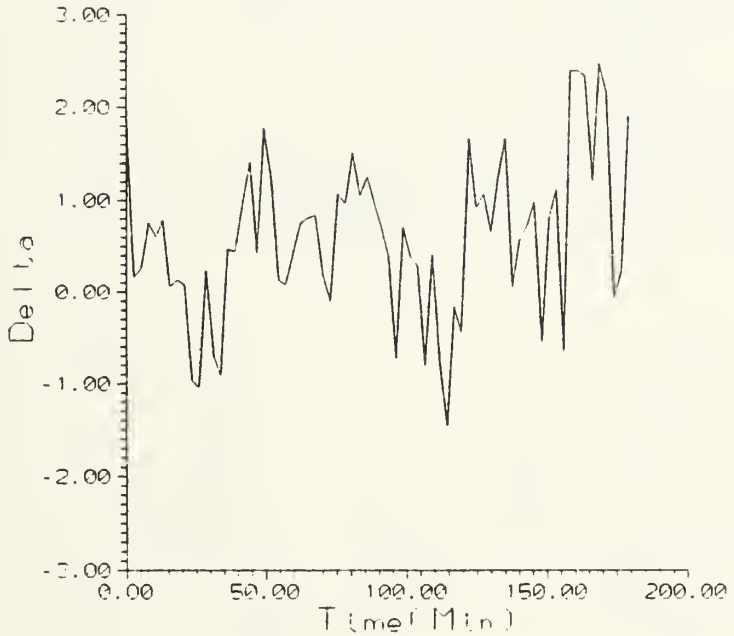

Figure 35. NOAA 10 1510Z 26 August 1992 Track FF Delta Ch 3.

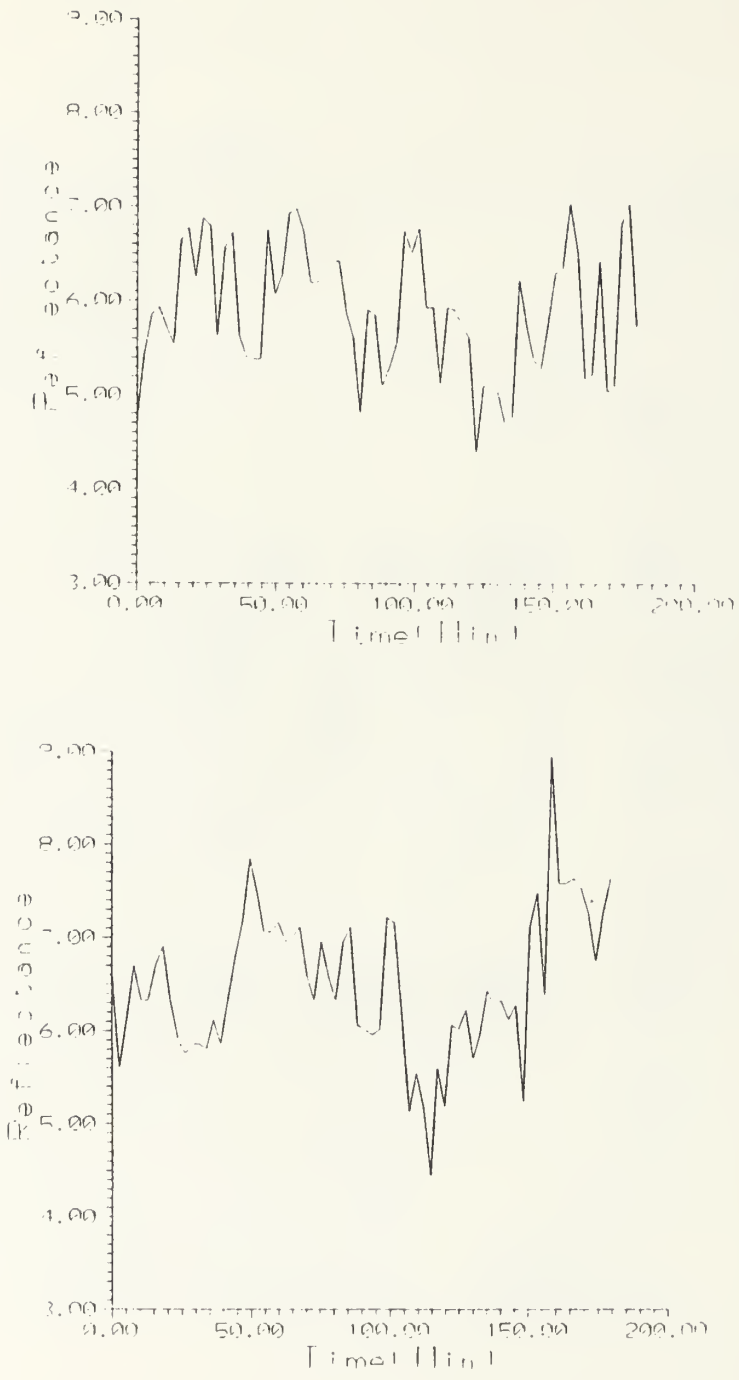

Figure 36. NOAA-10 1510Z 26 August 1992 Track UF Ambient Ch.3(Top) and Ship track Ch 3(Bottom).

Figure 37. NOAA-12 16357 26 August 1992 Track 11 Delta Ch.3(Top) and Track width(Bottom).

Figure 38. NOAA-12 1635Z 26 August 1992 Track 1F Ambient Ch.3(Top) and Ship-track Ch.3(Bottom)

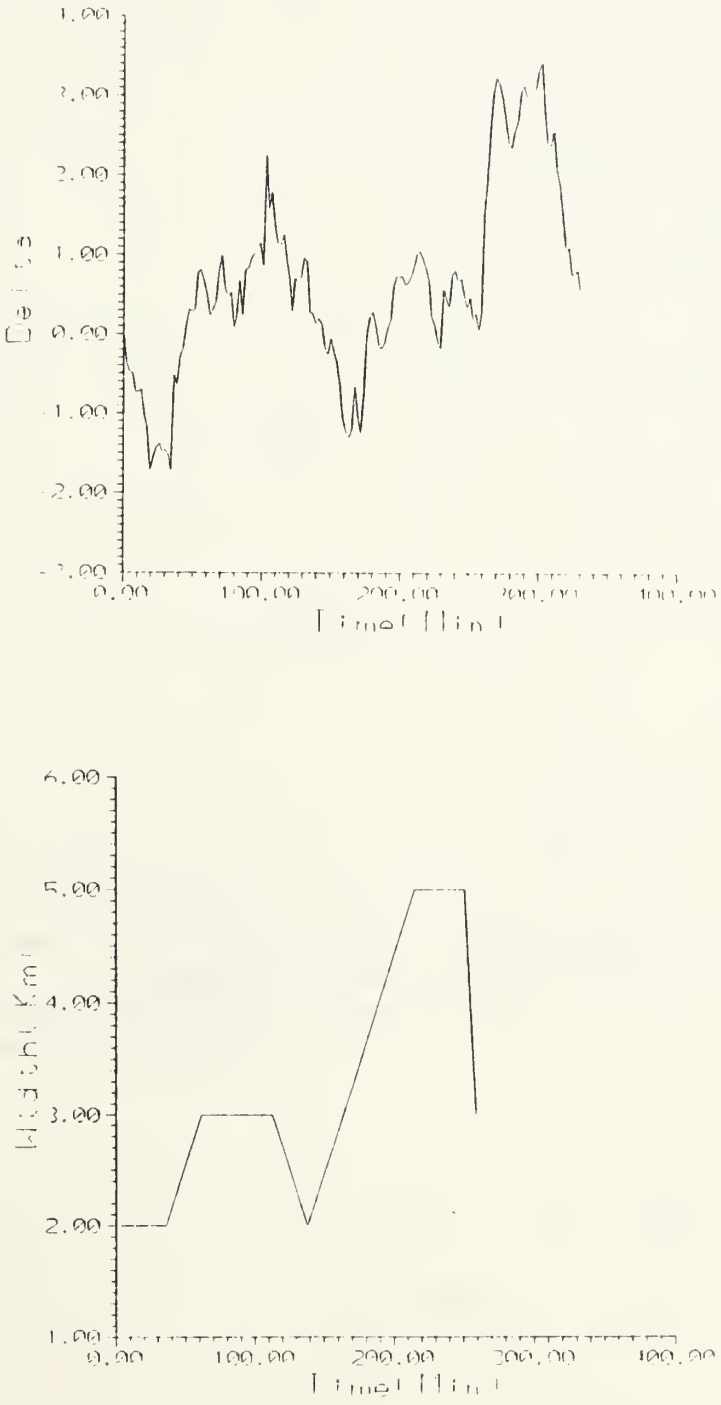

Figure 39. NOAA-11 22047 26 August 1992 Track Ht Delta Ch.3(Top) and Track width(Bottom).

Figure 40. NOAA-11 2201Z 26 August 1992 Track, EF Ambient Ch.3(Top) and Ship-track Ch.3(Bottom)

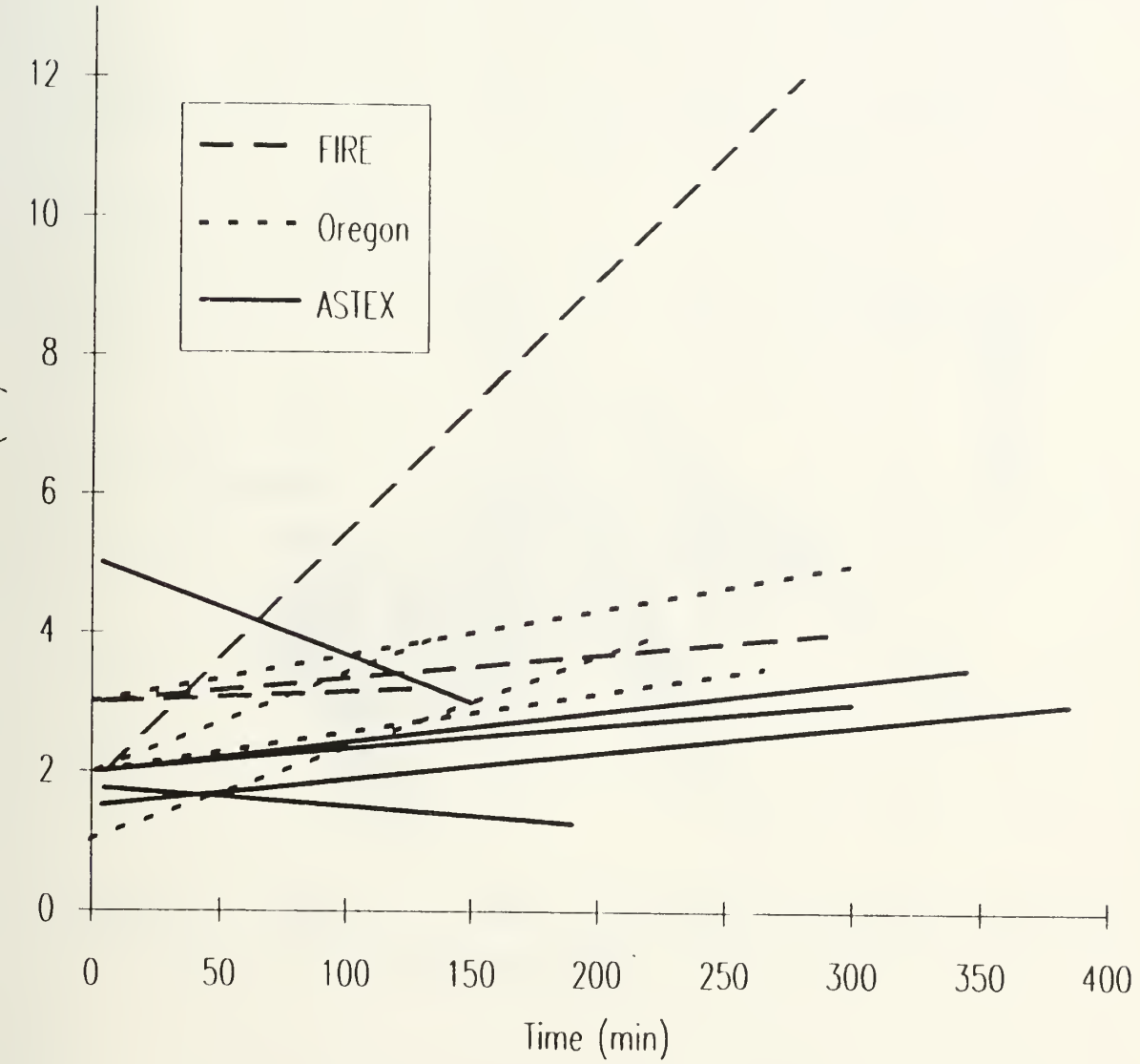

Figure 11. Composite of track width versus time

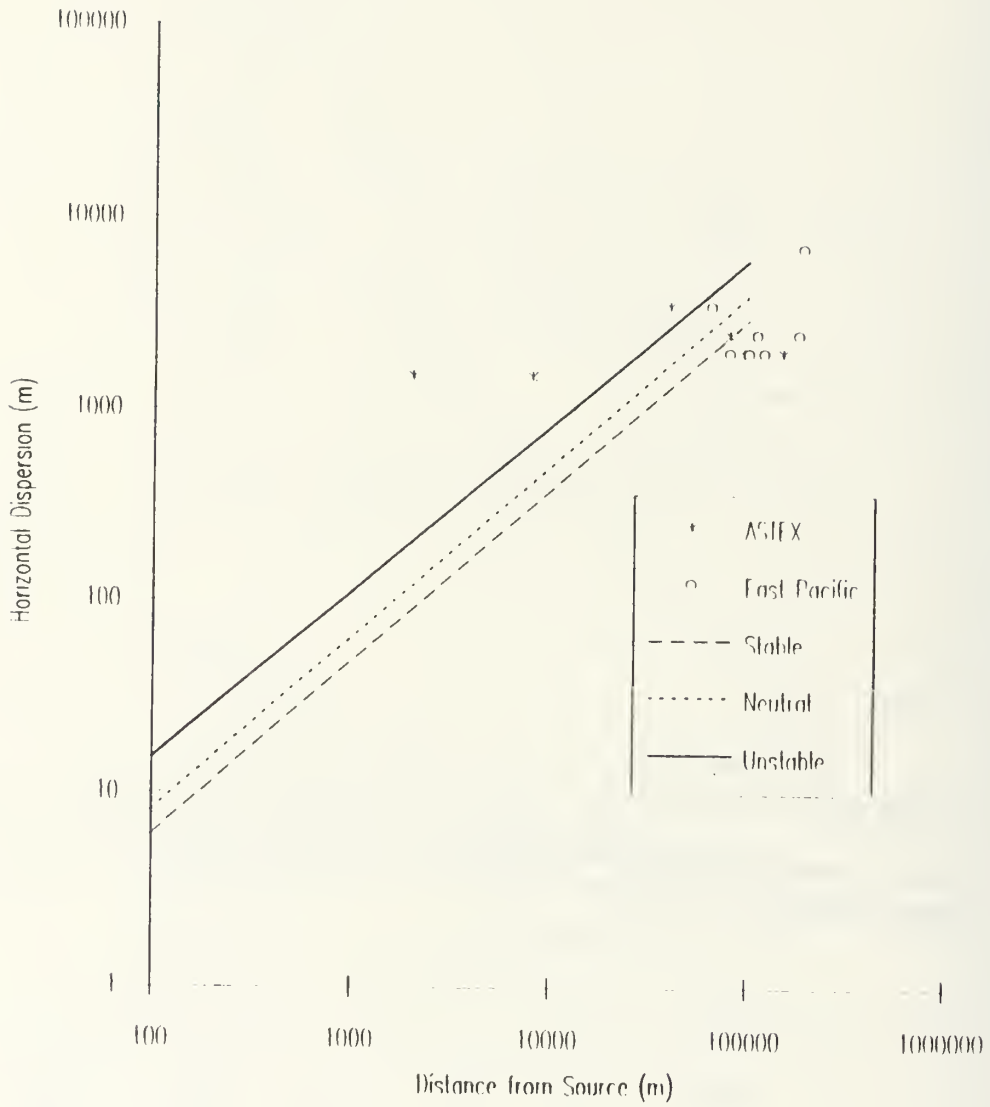

Figure 17. Pasquill-Gifford lateral dispersion coefficients with ASTEX and Eastern Pacific Ocean data.

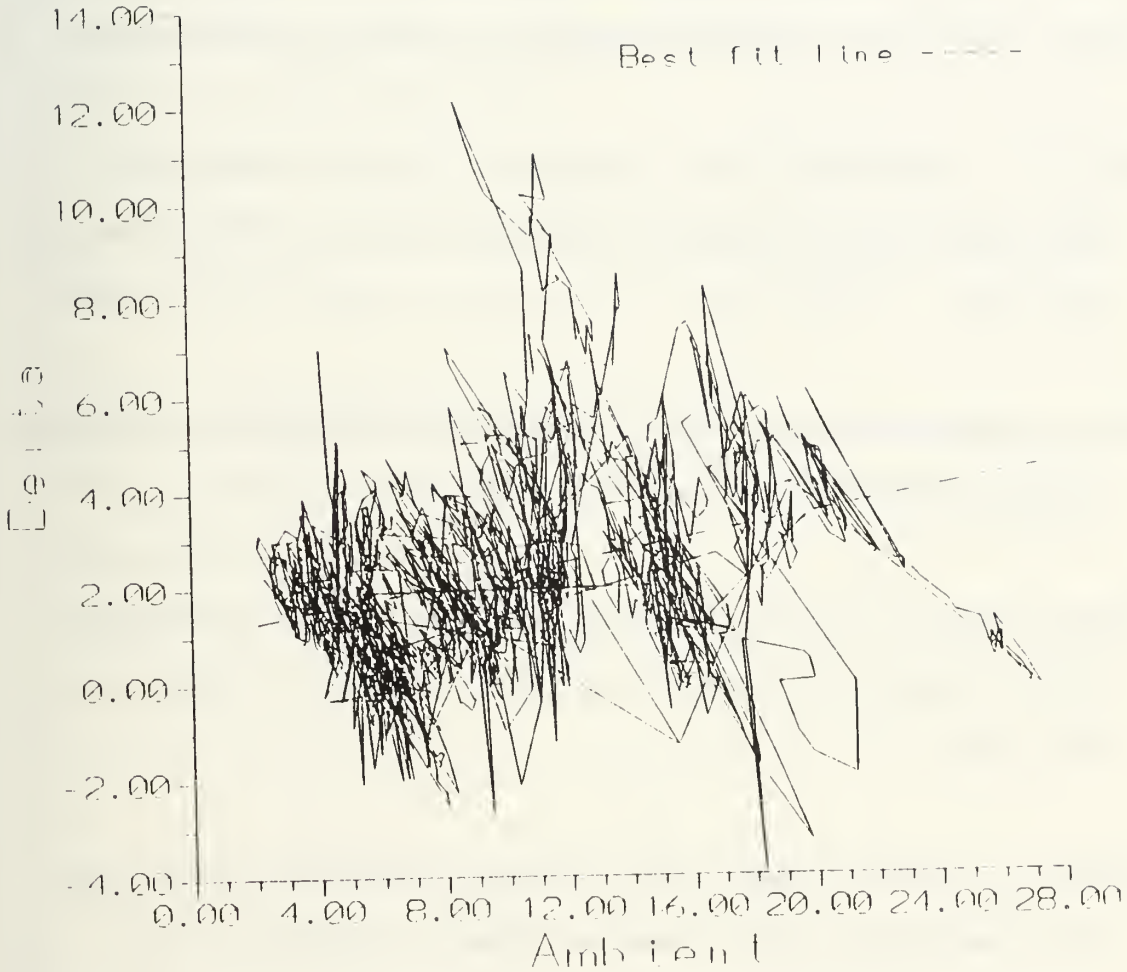

Figure 13. Composite of Delta reflectance versus ambient reflectance

LIST OF REFERENCES

Coakley, J.A., Jr., R. L. Bernstein and P. A. Durkee, 1987: Effect of ship stack effluents on cloud reflectivity. *Science*, **237**, 1020-1022.

Conover, J. H., 1966: Anomalous cloud lines. *J. Atmos. Sci.*, **23**, 778-785.

Dutton, J. A., and Panofsky, H.A., *Atmospheric Turbulence. Models and Methods for Engineering Applications*, pp. 241-243. John Wiley & Sons, Inc., 1984.

Freeberg, Mark. Natural Resources Consultant, Seattle Washington, Telefax. Subject: Vessel Descriptions. 10 November 1992.

Morehead, Steven, E., 1988: Ship track cloud analysis for the North Pacific area. M.S. thesis, Naval Postgraduate School, Monterey, CA, September 1988, 57 pp.

Nielsen, K. E. and P. A. Durkee, 1992: A robust algorithm for locating ship track cloud features using 3.7 micron satellite data. Preprints of Sixth conference on Satellite Meteorology and Oceanography, January 5-10, 1992, Atlanta, Ga, A. M. S. Boston, Ma. 1990.

Pettigrew, James. C., 1992: Surface meteorological parameters of identified ship tracks. M.S. thesis, Naval Postgraduate School, Monterey, CA. September 1992. 72 pp.

Salvato, Greg. 1992: Comparison between Arctic and subtropic ship exhaust effects on cloud properties. M.S. theses, Naval Postgraduate School. Monterey, CA. March 1992. 56 pp.

Starr, D. O., 1987: A Cirrus-Cloud Experiment: Intensive Field Observations Planned For FIRE. *Bull. Amer. Meteor. Soc.*, **68**, 119-124.

Twomey, S. and T. Cocks, 1982: Spectral reflectance of clouds in the near-infrared: comparison of measurements and calculations. *J. Meteor. Soc. Japan*, **60**, 583-592.

INITIAL DISTRIBUTION LIST

No. copies

1. Defense Technical Information Center — 1
   Cameron Station
   Alexandria, VA 22304-6145

2. Library, Code 52 — 2
   Naval Postgraduate School
   Monterey, CA 93943-5000

3. Chairman (Code MR/Hy) — 2
   Department of Meteorology
   Naval Postgraduate School
   Monterey, CA 93943-5000

4. Chairman (Code OC/Co) — 1
   Department of Oceanography
   Naval Postgraduate School
   Monterey, CA 93943-50000

5. Professor Philip A. Durkee (Code MR/De) — 1
   Department of Meteorology
   Naval Postgraduate School
   Monterey, CA 93943-5000

6. Professor Carlyle A. Wash (Code MR/Wx) — 1
   Department of Meteorology
   Naval Postgraduate School
   Monterey, CA 93943-5000

7. Mr. Bob Bluth — 1
   Naval Maritime Intelligence Center
   4301 Suitland Rd.
   Washington, DC 20395-5020

8. Oceanographer of the Navy 1
Naval Observatory
34th and Massachusetts Avenue NW
Washington, DC 20390-5000

9. Commander 1
Naval Oceanography Command
Stennis Space Center
MS 39529-5000

10. Dr. Dave Johnson 1
Office of Naval Research
Code 1243
800 N. Quincy St.
Washington DC 22217

11. Chief of Naval Research 1
Office of Naval Research
800 N. Quincy St.
Washington, DC 22217

12. Director of Naval Intelligence 1
The Pentagon Room 5C600
Washingto. DC 20350-2000

13..Mr. Mark Freeberg 1
Natural Resources Consultant, Inc. 4055 21st Avenue West
Seattle, WA 98199

14. LT. Tom Millman 1
U.S. Naval Oceanography Command Center
PSC 819, Box 31
FPO AE 09645-3200